telecom

Article

Carrier Frequency Offset Impact on Universal Filtered Multicarrier/Non-Uniform Constellations Performance: A Digital Video Broadcasting—Terrestrial, Second Generation Case Study

Sonia Zannou [1,†], Anne-Carole Honfoga [1,2,*,†], Michel Dossou [1,†] and Véronique Moeyaert [2,†]

1 Research Unit in Photonics and Wireless Communications (URPHORAN)/LETIA/EPAC, University of Abomey-Calavi (UAC), Abomey-Calavi 01 BP 2009, Benin; s.zannou@outlook.fr (S.Z.); michel.dossou@uac.bj (M.D.)
2 Electromagnetism and Telecommunications Unit (SET), Faculty of Engineering (FPMs), University of Mons (UMONS), 7000 Mons, Belgium; veronique.moeyaert@umons.ac.be
* Correspondence: anne-carole.honfoga@umons.ac.be
† These authors contributed equally to this work.

Abstract: Digital terrestrial television is now implemented in many countries worldwide and is now mature. Digital Video Broadcasting-Terrestrial, second generation (DVB-T2) is the European standard adopted or deployed by European and African countries which uses Orthogonal Frequency-Division Multiplexing (OFDM) modulation to achieve good throughput performance. However, its main particularity is the number of subcarriers operated for OFDM modulation which varies from 1024 to 32,768 subcarriers. Also, mobile reception is planned in DVB-T2 in addition to rooftop antenna and portable receptions planned in DVB-T. However, the main challenge of DVB-T2 for mobile reception is the presence of a carrier frequency offset (CFO) which degrades the system performance by inducing an Intercarrier Interference (ICI) on the DVB-T2 signal. This paper evaluates the system performance in the presence of the CFO when Gaussian noise and a TU6 channel are applied. Universal Filtered Multicarrier (UFMC) and non-uniform constellations (NUCs) have previously demonstrated good performance in comparison with OFDM and Quadrature Amplitude Modulation (QAM) in DVB-T2. The impact of CFO on the UFMC- and NUC-based DVB-T2 system is additionally investigated in this work. The results demonstrate that the penalties induced by CFO insertion in UFMC- and NUC-based DVB-T2 are highly reduced in comparison to those for the native DVB-T2. At a bit error rate (BER) of 10^{-3}, the CFO penalties induced by the native DVB-T2 are 0.96 dB and 4 dB, respectively, when only Additive White Gaussian Noise (AWGN) is used and when TU6 is additionally considered. The penalties are equal to 0.84 dB and 0.2 dB for UFMC/NUC-based DVB-T2.

Keywords: CFO; channel coding; DVB-T2; multicarrier modulation; UFMC NUC

Citation: Zannou, S.; Honfoga, A.-C.; Dossou, M.; Moeyaert, V. Carrier Frequency Offset Impact on Universal Filtered Multicarrier/Non-Uniform Constellations Performance: A Digital Video Broadcasting—Terrestrial, Second Generation Case Study. *Telecom* **2024**, *5*, 1205–1241. https://doi.org/10.3390/telecom5040061

Academic Editor: Peppino Fazio, Eirini Eleni Tsiropoulou, Carlos Tavares Calafate, Danilo Amendola

Received: 8 October 2024
Revised: 26 November 2024
Accepted: 29 November 2024
Published: 4 December 2024

1. Introduction

The Digital Video Broadcasting—Terrestrial, second generation (DVB-T2) standard constitutes the evolved version of Digital Video Broadcasting—Terrestrial, first generation (DVB-T) that meets the ever-growing demand of high-definition television (HDTV), ultrahigh-definition television (UHDTV), and mobile TV services. This standard has been adopted or deployed by most European and African countries. In particular as African countries took their time to migrate from analog to digital, going directly to the DVB-T2 system presents many advantages that were not considered in DVB-T. The DVB-T2 system includes the use of mobile reception services, the use of advanced channel coding techniques, and source coding methods, and the use of the concept of "Multiple Physical Layer Pipes" for data transmission [1]. All these DVB-T2 system advantages motivated researchers to have a significant interest into DVB-T2 system-related topics since its standardization in 2009 [2].

The multicarrier modulation technique defined in DVB-T2 is OFDM (Orthogonal Frequency-Division Multiplexing) that presents many benefits such as the reduction in the impact of Intersymbol Interference (ISI) and the increase in spectral efficiency in comparison with Single Carrier Modulation (SCM). However, it suffers from some drawbacks like synchronization problems and the reduction in spectral efficiency due to the insertion of a cyclic prefix (CP). These synchronization problems are accentuated by the presence of a carrier frequency offset (CFO) on the DVB-T2 signal at the receiver side. The CFO is defined as the frequency offset induced by the mobility of the receiver or by the frequency offset of the local oscillator. To estimate the CFO in a DVB-T2 system, P1 symbols are inserted at the beginning of each physical layer frames. A P1 symbol consists of three sections: the central section is generated by an inverse Fourier transform of a sequence of OFDM symbols, and the other two sections, added before and after the central one, respectively, are frequency-shifted repetitions of some samples of the central section and are viewed as guard intervals [3,4]. The central section is a 1K OFDM symbol that contains some basic Transmission Parameters Signaling (TPS) such as the FFT size and the Single-Input Single-Output (SISO)/Multiple-Input Multiple-Output (MIMO) mode [3]. Therefore, it cannot be considered as a training sequence since the signaling symbols used are a priori not known [4]. More accurate estimation methods have been proposed in the scientific literature during these last decades to increase the performance of the classical CFO estimator used in DVB-T2 [3–8]. The authors of [3] proposed an iterative double-detection CFO compensation technique and an ICI cancellation technique to deal with the double-phase errors encountered in the DVB-T2 environment's Single-Frequency Network (SFN) with the use case of the Multiple-Input Signal-Output (MISO) technique. In [4], the authors investigated on a robust timing and frequency synchronization method. A new P1 symbol with repetition and symmetrical conjugate correlation between the main part and the two guard intervals was proposed for DVB-T2 to improve the initial synchronization performance using the conventional P1 symbol. The authors of [5] presented a new subspace-based CFO estimator in OFDM that exploited both the dispersed and continuous pilots commonly used in mobile TV systems such as Digital Video Broadcasting—Handheld (DVB-H). This estimator was developed to cope with the high mobility, time slicing, and potential handovers during receiver deactivation time and was tested in a typical urban scenario. The authors of [6] proposed a modified version of the classic DVB-T2 estimator based on the characteristics of the P1 symbol. The performance of this new estimator was better than that of DVB-T2 in a practical channel environment. In [7], the authors proposed the time offset maximum likelihood (ML) and carrier frequency offset pseudo-maximum likelihood (PML) estimators that exploited the structure of the P1 symbol in the time and frequency domains for synchronization. The complexity of these estimators was analyzed. It was demonstrated that the ML was more complex than the PML estimator. The authors of [8] developed an effective symbol timing recovery (STR) that estimated the channel impulse response (CIR) using a scattered pilot (SP) pattern (existing in DVB-T2). The Fast Fourier Transform (FFT) properties were exploited to estimate the accurate symbol timing offset in a large delay channel environment with a MISO technique.

However, these studies do not present any details on the impact of the CFO increase on DVB-T2 system performance. Many of them only developed an efficient estimator for the DVB-T2 system. Therefore, a research gap is noticeable on the quantization of the CFO presence effect on the performance of this system.

Furthermore, many advanced multicarrier modulation techniques have been recently studied with the advent of 5G communication systems. These are Universal Filtered Multicarrier (UFMC), Filter Bank Multicarrier (FBMC), Generalized Frequency-Division Multiplexing (GFDM) and Filtered-Orthogonal Frequency-Division Multiplexing (F-OFDM) [9,10]. The specificity of these modulations is to add novel signal processing techniques to deal with OFDM's drawbacks. UFMC and FBMC performance has been mainly studied in DVB-T2 by comparing it to the classical OFDM performance. These modulation techniques present better BER performance without channel coding, and these outcomes are highly robust when channel coding techniques are used. In particular, UFMC distinguishes itself as the modulation that presents better performance than OFDM and FBMC as well as similar computational complexity when compared to OFDM [9,11]. Indeed, the specificity of DVB-T2 is to use a high number of subcarriers as a parameter, which increases the OFDM symbol duration and then allows the system to achieve better network coverage. However, as the number of subcarriers increases, the intercarrier spacing decreases. Thus, a deployed DVB-T2 network using a large number of subcarriers is more sensitive to frequency offset at the reception side than others using a small number of subcarriers.

Therefore, the study of the CFO impact in DVB-T2 system is relevant to support broadcasters planning to broadcast audiovisual signals for a mobile reception case. Furthermore, to the best of the authors' knowledge, the impact of the CFO has not yet been studied in UFMC in the framework of a DVB-T2 configuration. This paper is filling these gaps by evaluating the impact of CFO in both the native DVB-T2 system as a comparison basis and a UFMC-based DVB-T2 system. The main evaluation parameters are the bit error rate (BER), Modulation Error Ratio (MER), and Error Vector Magnitude (EVM) as these parameters are frequently used in digital signal measurement. However, no CFO compensation technique was developed in this document to eliminate the penalties induced by the presence of the CFO on the DVB-T2 signal.

The outline of this paper is as follows: the related works about this topic are firstly presented (cf. Section 2). It is followed by the theoretical background about multicarrier modulations and radiofrequency impairments (cf. Section 3). The material and methods are presented in Section 4. It is followed by the results (cf. Section 5) and a discussion (cf. Section 6). The paper ends with the conclusion (cf. Section 7).

2. Related Works

OFDM and UFMC are multicarrier modulations which have constituted a subject of research interest since the last decade. OFDM is mainly used in many communication systems such as DVB-T [12], DVB-T2 [2], Advanced Television Systems Committee, third generation (ATSC 3.0) [12], Visible-Light Communication (VLC) [13], 4G [14], and 5G [15]. A carrier frequency offset (CFO) is a radiofrequency impairment induced by an oscillator frequency mismatch between the transmitter and the receiver, also known as Doppler shift. This section presents the literature review.

2.1. Multicarrier Modulations in DVB-T2

This subsection presents papers that compare OFDM and UFMC performance in DVB-T2 and ameliorate DVB-T2 system performance by improving the signal processing techniques' robustness. It explains first the main improvements of the DVB-T2 system achieved by substituting the Orthogonal Frequency-Division Multiplexing (OFDM) modulation or the QAM constellation shaping techniques by other techniques. Second, it highlights some improvements gathered by enhancing any signal processing techniques like channel coding and MISO in DVB-T2.

Multicarrier modulations' (FBMC and UFMC) performance was investigated in DTT systems mainly in DVB-T and DVB-T2, as these systems are both based on OFDM, which presents some compatibilities with FBMC and UFMC. In 2020, filter-based waveforms (UFMC and FBMC) were studied, and their performance was compared to OFDM using DVB-T2 system parameters and its channel coding technique [9]. The numerical results proved that UFMC outperformed FBMC whose performance had previously been confirmed in DVB-T [16] and DVB-T2 systems [17] using BER after demapping and decoding. Furthermore, the spectral efficiency of these waveforms was studied and compared to the 100% OFDM spectral efficiency. With the aim of further improving system performance, the study of advanced constellations (NUCs) was carried out to replace the uniform constellation with a non-uniform constellation. The latter offers advantages in terms of Signal-to-Noise Ratio (SNR) improvement. In 2021, UFMC was jointly studied with a non-uniform constellation (NUC) in the framework of a DVB-T2 system. Indeed, Quadrature Amplitude Modulation (QAM) and OFDM are the modulations techniques used in DVB-T2 [18]. An advanced constellation shape technique called NUC was integrated in ATSC 3.0 as it presented better performance than the square shape constellation. In [18], this constellation was then inserted in both the native DVB-T2 and UFMC-based DVB-T2 systems to measure the impact. The main conclusion was that the UFMC NUC-based DVB-T2 system performance was really better than that of the native DVB-T2 system.

Filter-based multicarrier modulations offer better system performance. However, since they exploit the Fourier transform technique differently and incorporate a filtering step in their synoptic scheme, additional complexity could be added. Thus, during the same year, the same authors worked on the computational complexity of filter-based waveforms (FBMC and UFMC) proposed in the DVB-T2 context improvement [19]. The purpose of that study was to highlight the optimal low-complexity algorithm. Furthermore, the compromise between FBMC and UFMC waveforms applied to DVB-T2 in terms of SNR performance gains, spectral efficiency, and complexity was established. The results showed that UFMC was the waveform whose complexity could be reduced to OFDM complexity, and it presented a higher SNR performance gain with a reasonable spectral efficiency. It was demonstrated that parameters such as a number of subcarriers equal to 16384 and a cyclic prefix equal to one-fourth presented the larger CP overhead in DVB-T2. Using these parameters, UFMC was 128.51% spectrally more powerful than OFDM. These performance values were possible with UFMC as there was no need to add CP to achieve good BER performance, unlike OFDM. The previous works presented the DVB-T2 system performance improvement using filter-based multicarrier modulation. In the following works, the main outcomes using other techniques to increase system performance are presented.

In 2019, DVB-T2 system performance was investigated using Orthogonal Frequency-Division Multiplexing (OFDM) and realistic DVB-T2 channels [20]. A field measurement was first performed in urban areas such as Jakarta and Bandung cities to record transmission parameters and environmental parameters. These parameters were then inserted into the NYUSIM channel simulator to provide an instantaneous Power Delay Profile (PDP) with 1000 trials that allowed the authors to gather one representative PDP. These PDPs were exploited to evaluate the performance of DVB-T2 in Bandung and Jakarta using channel coding or not, with various transmission parameters. The results were useful to identify the optimal parameter on DVB-T2 technology.

In 2020, the performance of turbo channel coding were analyzed and compared to Low-Density Parity Check (LDPC) in DVB-T2 system [21]. The turbo decoder is an iterative decoder that presents the principle of a turbo engine. The system performance were evaluated first when turbo codes were used or not and second, when turbo codes and LDPC codes were compared. It was shown that LDPC codes presented better performance than turbo codes.

In the same year, instead of turbo codes applied in DVB-T2, the ML detector performance was evaluated in that system with a MIMO transmission scheme [22]. That detector's performance was analyzed when LDPC channel coding was applied or not. The Minimum Mean Square Error (MMSE) channel estimation method was used for the channel estimation. These performance values were evaluated in the case of an ideal channel estimation and the case of the MMSE estimation method. It was demonstrated that the channel response estimated by MMSE was not the same as the ideal channel response, leading to significant errors in the data received from the ML detector. When LDPC coding was applied, an efficient SNR improvement was observed.

In 2024, DVB-T2's performance was examined within High-Speed Train (HST) communication systems [23]. The main challenges were the high Doppler shifts and multipath effects management. The results proved that the error rates varied with speed and environmental conditions. The speeds considered during the simulation process were 10 m/s, 50 m/s, and 100 m/s. The CCDF, the Doppler effect, and the bit error number in excess were calculated for precise values of the mobile system's speed.

From all the above, we can see that the OFDM used in DVB-T2 has certain shortcomings. To overcome these shortcomings, several techniques are used, such as the MMSE channel estimation, the use of coding rates other than LDPC, etc. Other authors have proposed filtered-based multicarriers more efficient than OFDM.

2.2. CFO Case Studies in Multicarrier Modulations

A CFO results in Intercarrier Interference (ICI) by breaking the orthogonality between subcarriers. This part presents papers that investigated CFO case studies in multicarrier modulations and DVB-T2 in particular.

In 2006, a suboptimal scheme was proposed for OFDM systems to estimate the CFO using null subcarriers (i.e., subcarriers with no data transmitted) [24]. This scheme was based on the exploitation of one OFDM training sequence in which the use of odd subcarrier indexes like null subcarriers was imposed first and where even subcarriers indexes carried pilot tones. The work was performed assuming that the guard interval was longer than the Channel Impulse Response (CIR) length and the time synchronization was perfect. The specificity of that scheme was a reduced implementation complexity compared to previous work as the main required component was a simple correlator. Furthermore, null subcarrier allocation for the optimal maximum likelihood CFO estimation was also investigated using an extended m-sequence. It was demonstrated that that method presented improved performance compared to the previous one based on the principle of null subcarriers with distinct spacing.

In 2012, an optimum maximum likelihood (ML) synchronization method for P1 symbols was proposed [7]. Indeed, the P1 symbol was obtained in a similar way to that for an OFDM symbol. However, its features were different from a classical OFDM symbol and therefore were not really exploited by synchronization algorithms developed for multicarrier systems. The authors of that paper exploited the tripartite structure of the P1 symbol and the presence of null subcarriers in the vector transformed by an inverse Fourier transform. For the purpose of complexity reduction, ML synchronization for OFDM systems with no training sequence was used in parallel with the implementation of null subcarriers in OFDM symbols. Furthermore, the Cramér–Rao lower bound for the new scheme CFO estimator was investigated. That solution presented optimal performance while having a much lower complexity than that of the classical ML solution.

In the same year (2012), an ICI cancellation method was studied for a DVB-T2 system including the MISO technique [3]. Indeed, the P1 symbol inserted at the beginning of each T2 frame was used to estimate the CFO. That symbol presented a frequency-shifted guard interval at both ends which improved the correlation between the central part of the P1 symbol and the two intervals. Then, the estimation was performed by correlating the received P1 symbol and by recovering the argument of the correlator output's peak. When the MISO technique was exploited in DVB-T2, the signal and a slightly modified version of that signal were transmitted at the same time by two spatially separated transmitters having their own oscillators. That technique improved signal performance. However, two distinct CFOs, called dual CFOs, may appear in the received signal, one for each transmitter. In [3], the authors presented a method to mitigate Intercarrier Interference (ICI) occurring due to the dual CFOs after performing dual CFO compensation. They also proposed an iterative detection and ICI cancellation technique with the presence of a large CFO. Using that technique, the ICI was eliminated in a successive and iterative manner using the previously detected data samples and a priori LLR (Log-Likelihood Ratio) values fed from the LDPC decoder. The BER versus SNR simulation results showed that the proposed DVB-T2 receiver outperformed the case in which dual CFOs were perfectly known and came closer to the performance of the ideal dual-CFO-free case.

Moreover, CFO estimation techniques were presented, and their performance was evaluated using the Mean Square Error (MSE) [25]. The main estimation techniques presented were time-domain estimation (use of a cyclic prefix or training sequence) and frequency-domain estimation (pilot tone techniques). The simulation was performed using the CP-based technique, Moose (preamble-based techniques) and Classen (pilot-based techniques). The results showed that the Classen estimation technique was much more efficient than the other ones.

In 2015, the efficiency of OFDM systems with CFO estimation errors was measured in terms of spectral efficiency [26]. That work was performed regarding both the degradation in Signal-to-Interference-plus-Noise Ratio (SINR) due to the residual CFO, and the penalty of the extra power and spectral resources allocated to achieve the desired CFO estimation accuracy. Indeed, there still was a residual CFO after CFO estimation and compensation at the receiver which may degrade OFDM system performance. The authors of [26] presented a modified formula for the spectral efficiency of OFDM systems by making the trade-off between the following two conflicting factors related to the estimation-based CP and the training sequence method. Using too few training symbols induced an increase in CFO estimator errors while too many training symbols induced a loss of power and bandwidth system resources.

During the same year (2015), two ML CFO estimated methods called stochastic ML (SML) and deterministic ML (DML) were investigated by modeling the DVB-T2 transmitted signal as a stochastic and a deterministic unknown waveform, respectively, and assuming an unknown fading channel scenario [1] in contrast to the method developed in [4]. It was shown that the proposed deterministic ML method was more flexible and presented a lower computational complexity compared to the SML method but at the cost of reduced estimation accuracy. Numerical results demonstrated that both methods outperformed the cross-correlation-based method.

In 2016, the Symbol Error Rate (SER) versus SNR of UFMC and OFDM was evaluated in a 5G framework assuming the presence of a CFO or not and using mobile network system transmission parameters [27]. UFMC and OFDM performance was first compared. The results demonstrated that UFMC outperformed OFDM by 0.8 dB at an SER of 2×10^{-3}. Simulations were pursued, and it was demonstrated that the CFO estimator errors varied among these values: 10%, 20% and 50%. It was observed that for both OFDM and UFMC, the CFO estimation error critically diminished the SER performance of the system.

In 2017, other authors also studied UFMC and OFDM performance by evaluating the CFO impact on these multicarrier modulations [28]. Two different detection techniques such as Minimum Mean Square Error (MMSE) and Zero Forcing (ZF) were used. A simulation was performed by explicitly inserting a CFO on the receiver side and calculating the SER versus SNR. Single-user and multi-user UFMCs were investigated. Also, a MIMO technique was applied to the UFMC system. The results illustrated the good performance of UFMC when compared to OFDM without any CFO and with a CFO for a single user and multiple users in different communication environments.

In 2021, [29] explored the challenges in applying Orthogonal Frequency-Division Multiplexing (OFDM) to full-duplex (FD) cellular systems. This concerned the OFDM's vulnerability to interference due to frequency offsets. The authors compared FBMC with f-OFDM, UFMC, and GFDM.

In this section, related works about multicarrier modulations in DVB-T2 and CFO case studies in multicarrier modulations were presented. It was noticed that many papers presented CFO estimation and compensation algorithms in OFDM and DVB-T2. Only two papers addressed the impact of a CFO in OFDM and UFMC, respectively. Tables 1 and 2 summarize the papers by presenting their advantages and their limitations. Table 1 summarizes papers that studied multicarrier modulations in DVB-T2 and Table 2 summarizes papers that presented CFO case study in multicarrier modulations. To the best of our knowledge, there is no work that addresses the CFO impact on UFMC-based DVB-T2. This work fills this gap by evaluating the CFO impact on the received signal quality using UFMC- and NUC-based DVB-T2.

Table 1. Literature review (with advantages and limitations) on multicarrier modulations in DVB-T2.

Papers (Years)	Advantages	Limitations
[16] (2011)	Comparison of OFDM and FBMC using Brazil A (channel with line of sight—LoS) and Brazil D (channel without LoS) in DVB-T	Case of mobile reception not considered.
	BER versus SNR evaluated when channel coding (Reed Solomon and Convolutional code) was considered or not	MER and EVM tools were not used.
	FBMC 1-tap and 3-tap equalizers considered	Zero-forcing equalizer performance was not evaluated for FBMC; channel estimation method was not used.
[17] (2019)	Comparison of OFDM and FBMC using TU6 (urban environment) and 0 dB echo channel (Single-Frequency Network environment).	Case of mobile reception not considered.
	BER versus SNR evaluated when channel coding LDPC was considered or not. The system performance was evaluated using AWGN only and using fading channels.	MER and EVM tools were not used.
	CFIR 1-tap and 3-tap were considered for FBMC and zero-forcing equalizer is used for OFDM.	Zero-forcing equalizer performance was not evaluated for FBMC; channel estimation method was not used.
[9] (2020)	Comparison of OFDM with UFMC and FBMC using TU6 channel in DVB-T2	Case of mobile reception not considered.
	BER versus SNR evaluated when channel coding (LDPC) was considered or not. At a BER of 10^{-3}, UFMC gain was 1.2 dB, FBMC gain was 1 dB in comparison with OFDM.	MER and EVM tools and BCH code were not used. Channel estimation methods not used.
	Spectral efficiency of UFMC and FBM evaluated.	Computational complexity not really evaluated.
[18] (2020)	Comparison of NUCs' performance with QAM in DVB-T2. Comparison of UFMC and NUCs with OFDM and QAM using TU6 channel in DVB-T2.	Case of mobile reception not considered.
	NUCs from ATSC 3.0 standard was considered. BER versus SNR evaluated only when channel coding (LDPC) was considered. UFMC and NUCs jointly presented better performance than OFDM and QAM in DVB-T2.	MER and EVM tools and BCH code were not used. NUCs' constellations were not designed for DVB-T2 but were adapted for that system.
[19] (2021)	Literature review on filter-based waveforms' (FBMC and UFMC) implementation algorithms proposed for DTT systems.	There was no development of a complexity reduction algorithm.
	Complexity computation and analysis of FBMC and UFMC compared to OFDM.	The implementation of these algorithms was not performed in DVB-T2 but system parameters (number of subcarriers) were used to compute the complexity.
	Compromise between computation complexity and spectral efficiency was determined in order to choose a suitable algorithm.	The simulation time of each modulation was not evaluated in order to perform a complete analysis.
[20] (2019)	Radiofrequency profile establishment on the basis of field measurement parameters in an urban environment in Indonesia.	There was no consideration about Single-Frequency Network environments. The impact of environmental parameters on the establishment of the radio profile was not specified.
	Outage performance validation of DVB-T2 channels for the cities of Bandung and Jakarta were confirmed using the CP-OFDM system without channel coding (uncoded) compared to using channel coding repetition codes.	LDPC channel coding was not considered during simulation. Only BPSK modulation was used to validate performance. This modulation was more robust than DVB-T2 modulations such as 4-QAM, 16-QAM, 64-QAM, and 256-QAM. It was not really enough to conclude that the radio profiles generated were well suited to the DVB-T2 system.

Table 1. *Cont.*

Papers (Years)	Advantages	Limitations
[21] (2020)	Simulation and performance analysis of turbo coding implementation on the MIMO-based DVB-T2 system.	High constellation orders such as 64-QAM and 256-QAM usually used for rooftop antenna reception were not considered for the simulation.
	MMSE was used as the channel estimator.	Simulation was not performed when the Channel State Information (CSI) estimator was assumed to be perfect to assess the gap between the MMSE channel estimator performance and the ideal CSI estimator.
	Instead of a zero-forcing equalizer, a Vertical-Bell Laboratories Layered Space-Time (VBLAST) equalizer was used for the simulation.	ZF forcing equalizer was not considered in that work to highlight VBLAST performance in the presence of a DVB-T2 channel with MIMO.
[22] (2020)	Simulation and performance analysis of maximum likelihood detector on the MIMO-based DVB-T2 system with LDPC coding. That detector selected the symbol that had the closest Euclidean distance to the ideal symbol.	High constellation orders such as 64-QAM and 256-QAM usually used for rooftop antenna reception were not considered for the simulation.
	The impact of LDPC coding rate was highlighted when the coding rate increased. The ML detector showed better performance for lower coding rate using a BER performance evaluation tool.	There was no precision about the channel PDP used for the simulation. The external channel coding BCH was not considered for performance evaluation.
[23] (2024)	The application of High-Speed Train (HST) mobile speed in a DVB-T2 communication system was investigated. The impact of the Doppler frequency was considered.	There was no information about the impact of the transmission frequency variation on the Doppler frequency and DVB-T2 system performance.
	An HST channel environment was used for the simulation.	There was no detail about the CSI estimation method exploited.
	Doppler effects and bit error were analyzed using various speeds such as 10 m/s, 50 m/s, and 100 m/s, and the same transmission frequency equal to 700 MHz.	There was no analysis on the whole DVB-T2 frequency range. Only one frequency was considered for the simulation.

Table 2. Literature review on CFO case study (with advantages and limitations) in multicarrier modulations.

Papers (Years)	Advantages	Limitations
[24] (2006)	Used one OFDM training symbol instead of two symbols to perform the CFO estimation for which half of the symbols (odd subcarriers) included null-subcarriers.	The estimation range was limited within two subcarriers' spacing and should be extended.
	The use of some additional even null subcarriers reduced the computation complexity of the Fourier transform processing.	This even null subcarrier allocation was critical to the system performance.
[7] (2012)	Used the tripartite structure of P1 symbols to derive an optimum ML synchronization for P1 symbol	The P1 symbols were not known a priori by the DVB-T2 receiver. Therefore, in the presence of deep fading, the estimator should be limited.
	Two estimators such as ML and pseudo-ML were proposed. Their performance and their implementation complexity were compared.	DVB-T2 system performance was not evaluated using these estimators.
	Rayleigh channel and SFN fading channel environments were considered. The Cramér–Rao bound was estimated for both estimators.	TU6 channel and various SFN schemes were not considered. It was not performed for the SFN case as the CFO estimators were not suitable for the SFN environment.

Table 2. *Cont.*

Papers and Years	Advantages	Limitations
[3] (2012)	An iterative-detection dual-CFO compensation technique was proposed to deal with the dual phase errors experienced in a DVB-T2 MISO SFN environment.	The complexity of the technique was not evaluated.
	A successive-iterative ICI cancellation technique was also proposed to deal with the additional ICI introduced by the MISO technique in an SFN environment.	The complexity of the technique was not evaluated.
	The performance of both techniques was evaluated in DVB-T2 system using BER versus SNR when only the iterative-detection dual-CFO compensation was used and when they were both used.	Other performance evaluation tools like MER and EVM were not considered. The PDP of the MISO channel was not defined.
[25] (2012)	The numerical expression of Integer Frequency Offset (IFO) and Fractional Frequency Offset (FFO) were well developed.	The complexity of these techniques was not evaluated.
	CFO estimation techniques such as frequency- and time-domain techniques were presented in detail. The performance of CFO estimation techniques Classen and Moose was evaluated in OFDM transmission using BER versus SNR.	A trade-off between the performance of these techniques and their complexity was not obtained to choose the better technique.
[26] (2015)	The spectral efficiency of OFDM systems was evaluated in the presence of a residual CFO included in the signal after applying a CFO estimation technique.	The numerical expression of the SINR was derived but the relationship between SINR and spectral efficiency was not established.
	The spectral efficiency of cyclic prefix-based and training-based CFO estimators were evaluated and compared to the theory (Shannon capacity). The MISO transmission case was also considered.	PDP of the fading channel used for imperfect CSI case was not highlighted.
[1] (2015)	The stochastic and deterministic maximum likelihood (SML and DML) CFO estimation methods were derived using the special structure of the P1 symbol in DVB-T2 system. These algorithms were derived with the assumption that the CSI was unknown	The performance of these algorithms was not evaluated in the DVB-T2 system by using BER versus SNR. Only Cramér–Rao lower bounds and the Mean Square Error were used for the algorithms' performance. There was no information about the channel PDP used for simulation.
	The performance of these techniques was evaluated and compared to the previous estimation methods proposed in the literature. These algorithms could estimate the receive signal power, the time delays, and the CFO.	The complexity of these algorithms was evaluated by just evaluating the elapsed time of the proposed algorithms and comparing them to previous CFO estimation methods proposed.
[27] (2016)	The impact of the CFO on the UFMC system performance was evaluated and compared to those for OFDM.	There was a lack of justification of the CFO values used.
	A zero-forcing equalizer was used for both OFDM and UFMC. The Symbol Error Rate (SER) was the tool exploited for the performance evaluation	The channel PDP used was not highlighted.
[28] (2017)	The performance of single-user UFMC, multi-user UFMC, and MIMO-MU-UFMC systems was evaluated and compared to that of OFDM in the presence of a CFO.	There was a lack of justification of the CFO values used.
	Zero-forcing and MMSE equalizers were both used and their performance was compared. SER was the tool used.	The channel PDP used was not highlighted.

Table 2. *Cont.*

Papers and Years	Advantages	Limitations
[29] (2021)	FBMC was proposed as an alternative waveform to overcome the issue concerning the spectral leakage interference.	The channel estimation was complex when dealing with FBMC.
	That work proposed a detailed BER value comparison for OFDM, UFMC, FBMC, f-OFDM, and GFDM using full-duplex systems.	The proposed solution depended on high self-interference cancellation achievements, which could be difficult to achieve in a practical situation.

3. Theoretical Background

3.1. Multicarrier Modulations

Multicarrier modulation (MCM) defines a technique of transporting data over several subchannels of narrow bandwidth instead of conveying the data over the entire bandwidth in single-carrier modulation (SCM) schemes. MCM is known as a technique that uses multiple carrier signals at different frequencies, sending some of the bits on each subchannel. The main advantages of MCM are summarized as follows: its immunity to multipath fading channels (frequency-selective channels in particular), its enhanced immunity to Intersymbol Interference as the symbol period on each subchannel increases, its spectral efficiency, and its resilience to interference. Indeed, each subcarrier represents only a small portion of the total signal. If one subcarrier is lost or corrupted due to interference or noise, the overall signal remains almost intact. This resilience makes multicarrier modulation robust. OFDM is the most popular scheme used in digital video and audio broadcasting as well as Long-Term Evolution (LTE) downlink transmissions. However, UFMC modulation is proposed as an alternative for many communication systems including DVB-T2. This section presents these modulations and compares their features.

3.1.1. OFDM

The principle of OFDM is to group numerical data per package, and to modulate each piece of data by a different subcarrier at the same time. In this section, the OFDM block diagram is presented, and the numerical expression of the modulation is developed.

- Transceiver description
The OFDM transceiver scheme is presented in Figure 1. This modulation consists of three main steps: the symbol mapping, the Inverse Fast Fourier Transform (IFFT) processing (time-to-frequency-domain signal processing), and the cyclic prefix (CP) addition in emission. In reception, the steps are as follows: the CP cancellation, the Fast Fourier Transform (FFT) processing, and the symbol demapping. In DVB-T2, the symbol mapping method exploited is QAM. This mapping is performed on data containing redundant bits added by the LDPC Forward Error Correction (FEC) coder. After the mapping method in emission, the frequency-domain signal undergoes an IFFT operation which transforms the signal in a time-domain signal. The resulting signal is transmitted. The fading channel effects are applied to it. Also, AWGN is added to the signal obtained after the fading channel. In reception, an FFT operation is performed to convert the time-domain signal into a frequency-domain signal. As known, the CP and guard band include no useful data participating in the spectral efficiency reduction but allow one to reduce the Intersymbol Interference (ISI) and Adjacent-Channel Interference (ACI) impacts. Figure 2 shows the CP insertion process. T_{CP} denotes the CP duration. The OFDM symbol duration is extended using the CP, which represents the copy of a part of the OFDM symbol at the starting point of each symbol.

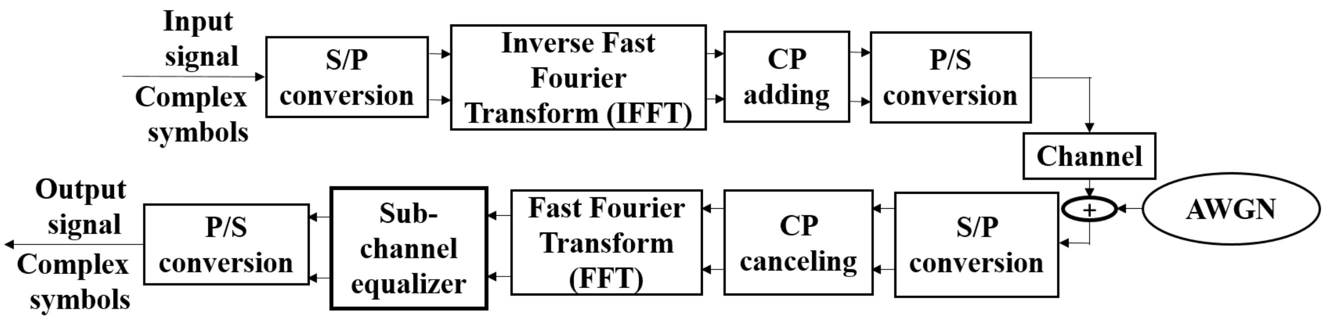

Figure 1. CP-OFDM transceiver block diagram.

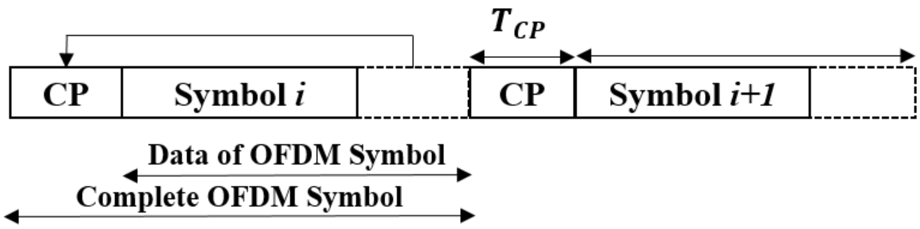

Figure 2. CP insertion.

- Numerical signal expression

  The numerical development is performed by assuming complex data symbols named $c_k \in (c_0, c_1, c_2, ..., c_{N_{FFT}})$. These data are QAM symbols formed by the grouping of n bits. The sequence of data normally undergoes an IFFT process. Let us assume that N_{FFT} is the number of OFDM subcarriers, and the time period T_s separates two sequences of N_{FFT} data. T_s is equal to one OFDM symbol duration. k is a positive integer ($k \in (1, ..., N_{FFT})$). During the modulation process, each c_k is modulated at the high frequency f_k. Each individual signal is then expressed in a complex form as the multiplication of c_k by $e^{2j\pi f_k t}$. Therefore, the main signal $x(n)$ corresponding to the total N_{FFT} data is shown as follows:

$$x(n) = \sum_{k=0}^{N_{FFT}} c_k.e^{j2\pi f_k n} \tag{1}$$

  As the main peculiarity of OFDM is the orthogonality between subcarriers (orthogonal multiplexing), thus the subcarrier spacing is inversely proportional to the symbol period and is equal to $\frac{1}{T_s}$. If we denote f_0 the carrier frequency, $f_k = f_0 + \frac{k}{T_s}$. Then, $x(n)$ can be expressed as:

$$x(n) = e^{j2\pi f_0 n} \sum_{k=0}^{N_{FFT}} c_k.e^{2j\pi \frac{kn}{T_s}} \tag{2}$$

3.1.2. UFMC

The UFMC technique overcomes the limitation of the OFDM by adding generalized pulse-shaping filters that ensure the frequency- and time-domain spectral localization. Its main characteristics are (1) the use of sub-band filtering instead of subchannel filtering in FBMC, (2) the whole band filtering in F-OFDM, and (3) the exploitation of a complex data symbol as in OFDM.

- Transceiver description
The UFMC transceiver scheme is illustrated in Figure 3. As shown, QAM data symbols are divided into sub-groups that undergo IFFT processing separately and are filtered using a sub-band filtering technique. The filter prototype used is the Finite Impulse Response (FIR) Dolph–Chebyshev filter of length L. The aim of introducing an FIR filter to filter each sub-band is to reduce the Out-Of-Band (OOB) spectrum. All results from the sub-group data processing are summed up and therefore constitute the UFMC symbol. This symbol is transmitted through the fading channel, and AWGN is added to the signal. At the receiver side, a zero-padding technique is used to fill the data of length $N_{FFT} + L - 1$ with $N_{FFT} - L + 1$ zeros samples to reach a length of $2 \times N_{FFT}$. The purpose of this zero-padding technique is to exploit the FFT processing and filter properties to recover data [9]. Therefore, the FFT technique is applied to pass data from the time domain to the frequency domain. After that, a downsampling technique is applied to recover one sample out of two on all $2 \times N_{FFT}$ samples. Finally, the same subchannel equalizer (as applied in OFDM) is also applied on the recovered data to retrieve QAM data symbols.

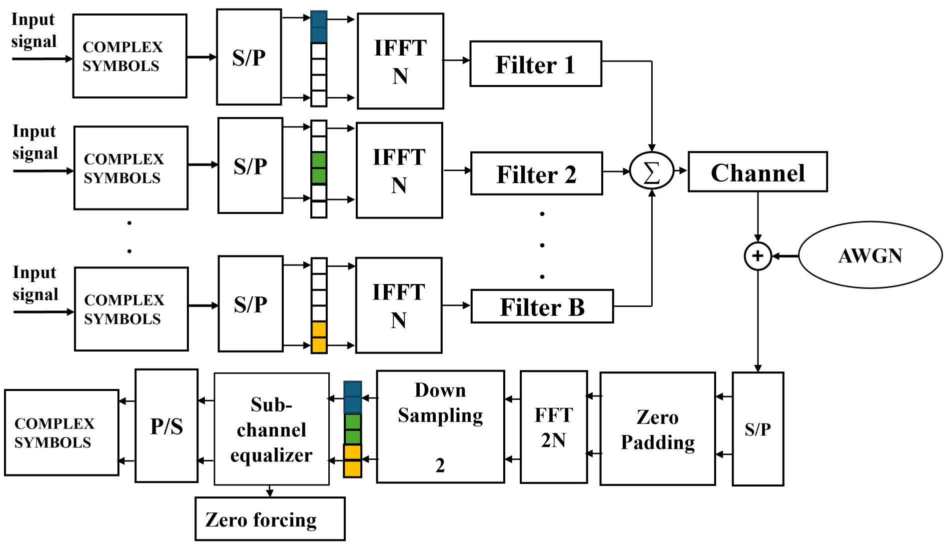

Figure 3. UFMC block diagram.

- Numerical signal expression
Suppose that $B * n_i$ represents complex data symbols resulting from QAM baseband modulation. As previously presented, the full band of N subcarriers is partitioned into B sub-bands. The number of subcarriers in each sub-band is fixed (n_i complex QAM symbols). In the transmitter section, to cancel sub-band interference, IFFT processing is employed to transform the frequency-domain signal into a time-domain signal. At each N_{FFT} point, sub-bands are computed, and zeros are attributed to unreserved subcarriers. The filtering operation is applied by performing a linear convolution between data IFFT processing and the filter components. The time-domain transmission x vector (at the input of the channel) for a particular multicarrier symbol is the superposition of the sub-band-wise filtered components, with filter length L and FFT length N_{FFT} (for simplicity, the time index m is dropped) [30]:

$$x_{(N_{FFT}+L-1)\times 1} = \sum_{i=1}^{B} F_{i_{(N_{FFT}+L-1)\times N_{FFT}}} \times V_{i_{N_{FFT}\times n_i}} \times S_{i_{n_i \times 1}}; \tag{3}$$

For each of the B sub-bands, indexed i, the n_i complex QAM symbols gathered in S_i representing a frequency-domain signal are converted to a time-domain signal by the IFFT-matrix V_i. V_i includes the relevant columns of the inverse Fourier matrix in accordance with the respective sub-band position within the overall available frequency range. F_i is a Toeplitz matrix, composed of the filter impulse response which is used to perform the linear convolution.

3.2. Non-Uniform Constellations

In DVB-T2 system, the uniform QAM constellation scheme is exploited. This constellation is a two-dimensional rectangular constellation generally defined by the uniform spacing between constellation symbols. The different constellation symbol numbers, also called valence, are 4, 16, 64, and 256. However, the most robust modulation against noise and channel uniform constellation is 4-QAM (QPSK). The main specificity of the scheme used in DVB-T2 is the Gray mapping technique, whose goal is to minimize the bit error probability since the Hamming distance between two adjacent symbols is equal to one. Furthermore, the advances in scientific research have given rise to new constellation schemes. There are rotated constellations already proposed in DVB-T2 and non-uniform constellations (NUCs) proposed in ATSC 3.0. While the former has shown better performance in the presence of a frequency-selective channel, the latter's performance is really highlighted mainly when only Gaussian noise is used and also when the Gaussian noise and a frequency-selective channel are present during transmission. Using these constellation shapes, it has been demonstrated that ATSC 3.0 standard performance is better than that of DVB-T2 [31]. Also, it represents the standard closer to the Shannon Limit. Two shapes of non-uniform constellations (NUCs) are defined: one-dimensional NUCs (1D-NUCs) maintain the rectangular shape of uniform constellations and relax the uniformity constraint; the two-dimensional NUCs (2D-NUCs) break the uniformity constraint as they present a circular shape. They present better performance than 1D-NUCs. During the 2D-NUC constellation design, the constellation values can take any shape inside one quadrant, and the other three quadrants are derived from the first quadrant by symmetry [32]. In this paper, 2D-NUC developed in ATSC 3.0 was retained for the CFO performance evaluation in the DVB-T2 system as its performance was previously shown in [18]. Various shapes of constellations were designed by combining a constellation size and code rate of the LDPC channel coding. The 2D-NUC that matched the DVB-T2 parameters with 16-QAM and a CR of one half was the 8/15 2D-NUC (page 186, [33]).

3.3. Radiofrequency Impairment: CFO

Various kinds of radiofrequency (RF) impairments exist in wireless communication systems. There are thermal and flicker noises, local oscillator phase noise, sampling jitter, Digital-to-Analog Converter (DAC) and Analog-to-Digital Converter (ADC) quantization noise and clipping, quadrature imbalance, carrier frequency offset (CFO), and sampling frequency offset (SFO) [34]. As previously discussed in the introduction, multicarrier systems are sensitive to synchronization errors. They induce system performance degradation. This deterioration increases with the number of subchannels. As the DVB-T2 system includes a high number of subcarriers (1024, 2048, 4096, 8192, 16,384, and 32,768), it constitutes a subject of interest to evaluate the impact of carrier frequency offset (CFO) on the system performance. The description of the CFO is presented in the following part.

- CFO description
  Generally, in communication systems, the carrier frequencies are generated from frequency synthesizers, commonly Phase-Locked Loops (PLLs), using precise crystal oscillators whose performance is specified with a certain precision in parts per million (ppm) [34]. The CFO refers to the deviation in the actual receiver carrier frequency (RX carrier frequency) from the nominal carrier frequency (TX carrier frequency) in these systems. This frequency offset is caused by two factors. The first factor is the Doppler shift due to the relative mobility of the transmitter and the receiver (and even the channel), and the second one is the difference between the frequencies of the local oscillators at the transmitter and receiver. As DVB-T2 system represents the case study, only the receiver is mobile. The transmitter is fixed in the terrestrial digital broadcasting system. The CFO impact has to be evaluated in two different cases:

when only Gaussian noise is used and when a fading channel and Gaussian noise are used together; the OFDM system including frequency offset models are presented in Figures 4 and 5, respectively.

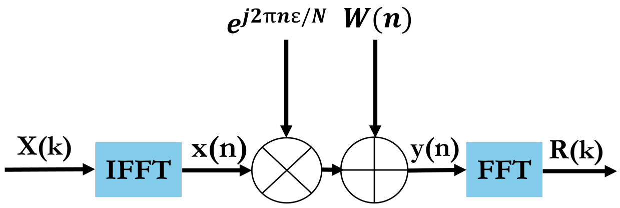

Figure 4. OFDM modulation with frequency offset model: Gaussian noise only.

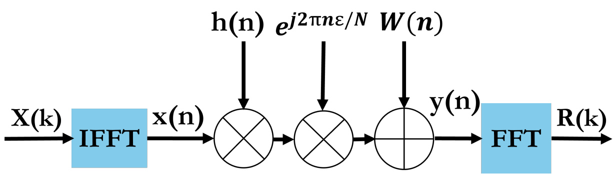

Figure 5. OFDM modulation with frequency offset model: fading channel and Gaussian noise only.

Let us assume that the carrier frequency offset does not change between two consecutive symbols. The received y(n) OFDM symbol when only Gaussian noise is considered and when fading channel and Gaussian noise are considered can then be expressed as Equations (4) and (5), respectively.

$$y(n) = x(n) \times e^{\frac{j2\pi n\epsilon}{N_{FFT}}} + W(n) \tag{4}$$

$$y(n) = \sum_{\Gamma=0}^{\tau-1} x(n-\Gamma) \times h(\Gamma) \times e^{\frac{j2\pi n\epsilon}{N_{FFT}}} + W(n) \tag{5}$$

$$\epsilon = \Delta f \times N_{FFT} \times T_{sampling} = \frac{\Delta f}{f_1} = \Delta f \times T_s \tag{6}$$

$$\Delta f = |f_{crx} - f_{ctx}| \tag{7}$$

– x(n) is the time-domain OFDM transmitted symbol.
– y(n) is the received OFDM symbol.
– ϵ is the normalized frequency offset given by Equation (6) [34]. Δf represents the frequency difference between the transmitter and the receiver. $T_{samping}$, f_1, T_s, and N_{FFT} are, respectively, the sampling period, the OFDM subcarrier spacing, the OFDM symbol period, and the whole number of subcarriers.
– W(n) is the Gaussian noise signal added to the frequency shifted signal
– h(n) is the channel impulse response of length τ

The OFDM symbol period is computed using Equation (8), where f_1 is defined in Equation (9). $F_{sampling}$ is the frequency sampling defined in DVB-T2 using Equation (10) [35]. It depends on the channel bandwidth B.

$$T_s = \frac{1}{f_1} \tag{8}$$

$$f_1 = \frac{F_{sampling}}{N_{FFT}} \tag{9}$$

$$F_{sampling} = \frac{64}{7} \times \frac{B}{8} \tag{10}$$

When a fading channel is considered during signal transmission, a convolution operation is applied between each OFDM symbol and the channel impulse response (cf. Equation (5)).
The normalized CFO (ϵ), defined in Equation (6), becomes Equation (11).

$$\epsilon = \frac{\Delta f}{f_1} = \Delta f \frac{N_{FFT}}{F_{sampling}}$$
$$\epsilon = \frac{\Delta f}{f_1} = \Delta f \frac{N_{FFT}}{\frac{64}{7} \times \frac{B}{8}} \quad (11)$$

As previously presented, the main impact of the CFO on the OFDM subcarrier is the presence on Intercarrier Interference (ICI) between the main subcarriers and the adjacent subcarriers. Figures 6 and 7 show a comparison without and with the CFO, respectively, after the Fast Fourier Transform operation performed at the receiver side [34]. The greater the CFO value is, the more intense the ICI between subcarriers. Then, the ICI increases with the number of subcarriers used per OFDM symbol transmission, as the subcarrier spacing value diminishes when the number of subcarriers increases.

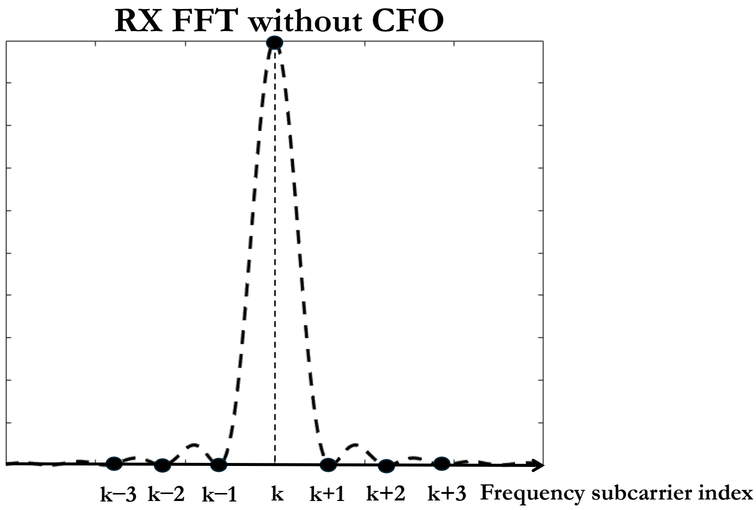

Figure 6. OFDM subcarriers without CFO—adapted from [34].

- Doppler effect case study In the case of the receiver mobility, a Doppler shift affects the signal frequency and then the OFDM subcarriers. According to the moving direction and the various speeds of the receiver, the values of the Doppler shift vary, inducing a transmitter frequency decrease or increase [36]. Figure 8 presents an illustration of the Doppler effect when the receiver is moving. Let us use the following notations:
  - Δf_D is the Doppler shift, which is also the frequency difference between the transmitter frequency and the receiver frequency, previously called Δf.
  - v is the vehicle speed, which varies (m/s).
  - f_0 is the transmitter frequency (Hz).
  - c is the speed of light (electromagnetic wave) ($3 \times 10^8 m/s$).
  - φ is the angle between the direction of motion and the line of sight to the transmitter ($0 < \varphi < \pi$).

$$\Delta f_D = v \times \frac{f_0}{c} \times \cos(\varphi) \quad (12)$$

There are three specific cases of Doppler shift:

  - Case 1: the vehicle is moving towards the transmitter, so $0° < \varphi < 90°$, i.e., $1 > \cos(\varphi) > 0$, and finally $\Delta f_{D_{max}} > \Delta f_D > 0$.

– Case 2: the vehicle is moving away from the transmitter, so $90° < \varphi < 180°$, i.e., $0 > \cos(\varphi) > -1$ ($\cos(\varphi)$ is negative), and finally $0 > -\Delta f_D > -\Delta f_{D_{max}}$.
– Case 3: the vehicle is driving around the transmitter in circles; $\varphi = 90°$, $\cos\varphi = 0$, and the transmit frequency remains unchanged.

To conclude, the Doppler shift is directly proportional to the carrier frequency f_0 of the transmitter. Considering the same OFDM mode (number of subcarriers), the lower the frequency f_0, the smaller the Doppler effect. Hence, the OFDM subcarrier spacing is weakly affected. Conversely, the higher the frequency f_0, the larger the Doppler effects. Hence, the OFDM subcarrier spacing is highly affected.

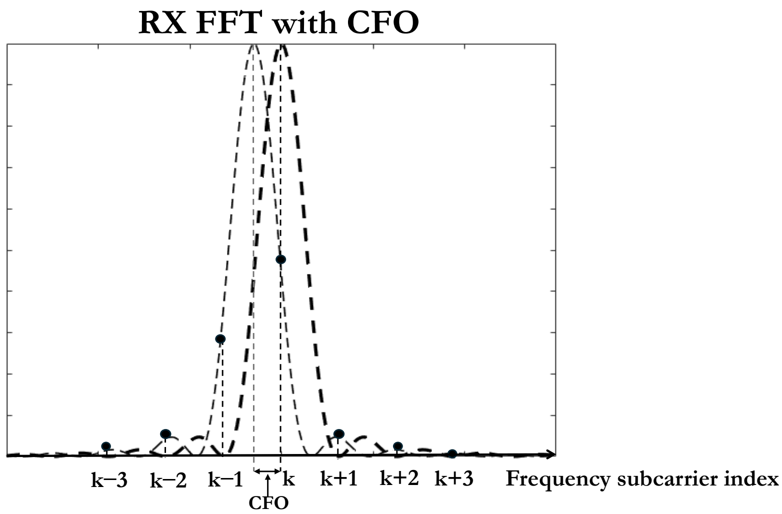

Figure 7. CFO impact on subcarriers—adapted from [34]. The black curve represents the expected subcarrier curve at the receiver, and the gray curve represents the subcarrier curve at the receiver with a frequency offset (CFO).

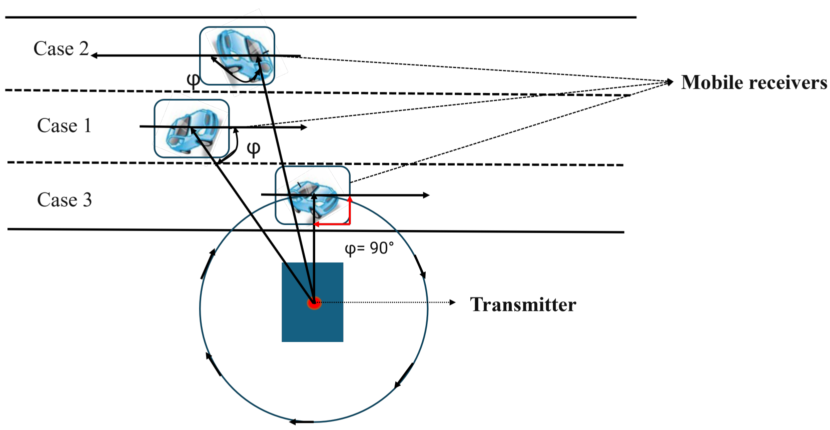

Figure 8. Doppler effect.

From all the above, the normalized CFO expression is defined, assuming the DVB-T2 transmission parameters in Equation (13).

$$\epsilon = v \times \frac{f_0}{c} \times \cos(\varphi) \times \frac{N_{FFT}}{\frac{64}{7} \times \frac{B}{8}} \quad (13)$$

The maximum value of the Doppler shift is achieved when $\cos(\varphi)$ is equal to ±1. The absolute value of the Doppler shift is then computed. If the maximum Doppler shift is considered, then the normalized CFO (ϵ) is equal to the expression in Equation (14).

$$\epsilon = v \times \frac{f_0}{c} \times \frac{N_{FFT}}{\frac{64}{7} \times \frac{B}{8}} \tag{14}$$

4. Material and Methods

In this section, a light version of the DVB-T2 system is developed and a simulation is performed using Matlab software. The main steps of the simulation, the systems implemented, and the parameters used are presented.

4.1. Simulation Steps

A DVB-T2 system includes many processing blocks, and only the main blocks were implemented in our simulator, the native DVB-T2 system implemented was the light version of DVB-T2. Three main performance evaluation tools such as the BER, MER, and EVM were used in this work. The main simulation steps exploited to evaluate CFO performance are highlighted in Figure 9.

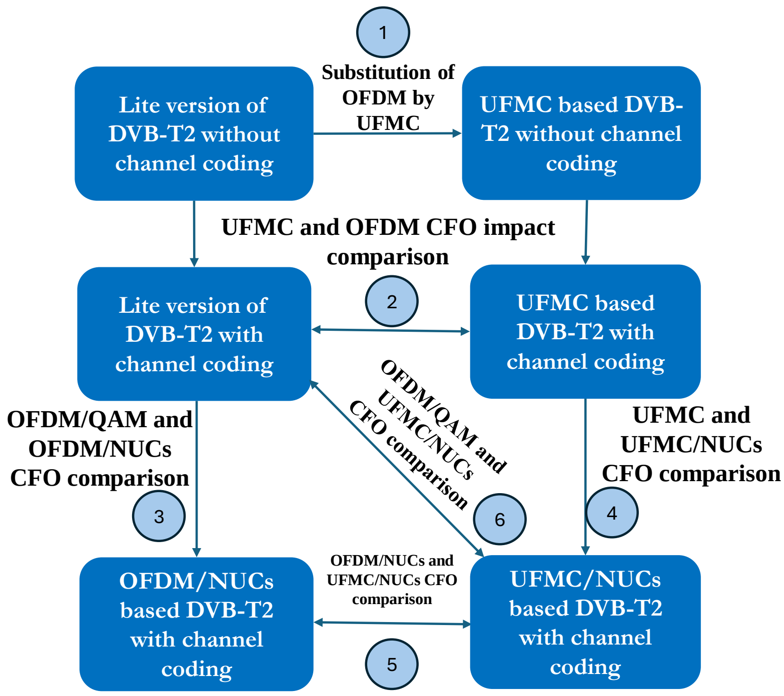

Figure 9. CFO evaluation process in two cases: Gaussian noise and Gaussian noise with a TU6 fading channel.

As shown in this figure, the first step (1) was the development and simulation of the light version of the DVB-T2 system called native DVB-T2 and the Universal Filter Multicarrier (UFMC)-based DVB-T2 system and the CFO insertion. The second step (2) consisted in adding LDPC coding in both systems and evaluating the CFO impact. The third step (3) consisted in substituting the QAM mapping block for a 2D-NUC block in both the native DVB-T2 transmitter and the receiver. The fourth step (4) performed the same task as the previous one, but an NUC was inserted in the UFMC-based DVB-T2. The fifth step (5) consisted in comparing the CFO impact in the NUC-based DVB-T2 system to the CFO impact in Universal Filter Multicarrier/non-uniform constellation (UFMC/NUC)-based DVB-T2 system, and the last step (6) consisted in comparing the CFO impact on the native DVB-T2 system to the CFO impact on the UFMC/NUC-based DVB-T2 system. It is relevant to remember that simulations were performed when only Gaussian noise was considered and when both Gaussian noise and a fading (TU6) channel were used.

4.2. Implemented Systems and Simulation Parameters

Figure 10 exhibits the implemented system using Matlab. Since we dealt with digital transmission, binary data were transmitted, and a random binary data generator was used for the data generation. These data underwent the main signal processing techniques such as LDPC channel coding, QAM mapping, and OFDM modulation. The signal gathered passed through the Typical Urban 6 channel model, and Gaussian noise was added. As already highlighted in Section 3.3, a CFO was included in the signal according to the simulation cases such as the simulation without a fading channel and the simulation with a fading channel. The reverse operations were then performed at the receiver side.

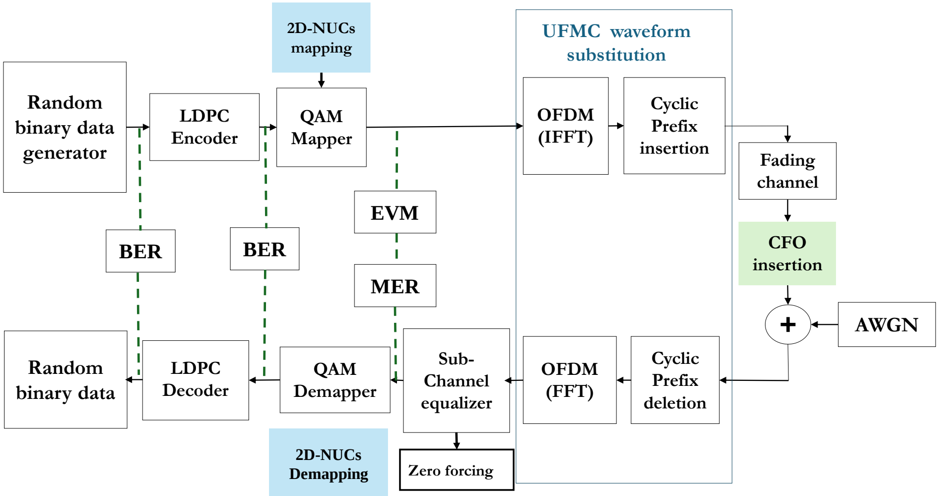

Figure 10. Light version of the DVB-T2 system: QAM substitution by NUCs and OFDM substitution by UFMC; CFO insertion.

Moreover, the CFO impact was also evaluated when QAM mapping and OFDM were substituted by 2D-NUC mapping and UFMC, respectively. Figure 11 presents the detailed UFMC/NUC-based DVB-T2 system. The process of CFO insertion was performed before the AWGN adding process.

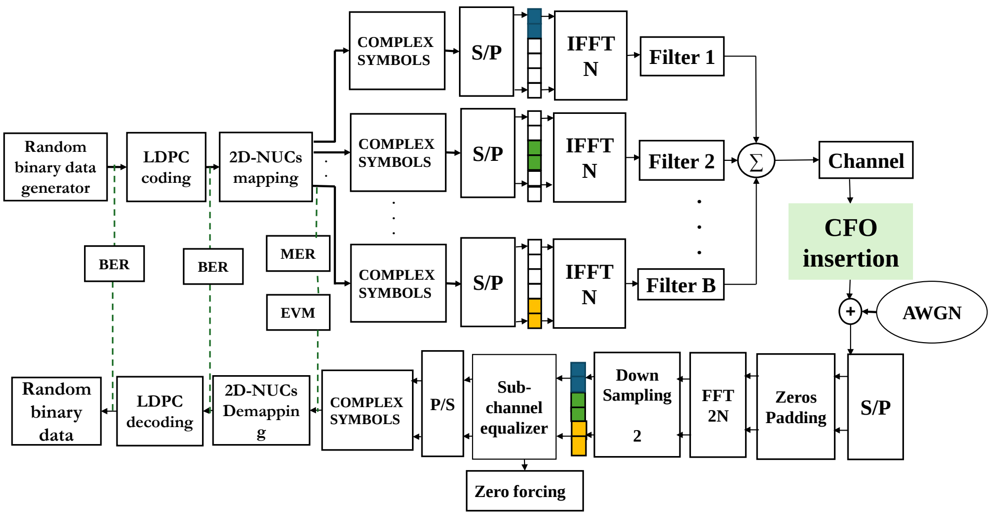

Figure 11. UFMC/NUC-based DVB-T2 system: CFO insertion.

The parameters used for all simulations are presented in Table 3. Simulations were carried out assuming perfect channel estimation. While the number of subcarriers and the cyclic prefix were useful in OFDM, in UFMC, the number of subcarriers, the filter length, the sub-band bandwidth, the sub-band number, and the sub-band offset were the useful parameters.

Table 3. Simulation parameters.

Parameters	Values
Channel bandwidth B	8 MHz
Transmission frequency f_0	474 MHz
Vehicle speed v	50 km/h (13.88 m/s) to 150 km/h (41.66 m/s)
Normalized CFO	0.01, 0.02, 0.03, 0.04, 0.05
OFDM subcarrier number N_{FFT}	8192
OFDM cyclic prefix	1/32
OFDM symbol duration	896 µs
OFDM subcarrier spacing	1116.07 Hz
Constellation size	16
Number of bits per symbol QAM	4
LDPC frame length	64,800
LDPC code rate	1/2
LDPC Matlab function	dvbs2ldpc (parity check matrix) comm.LDPCEncoder (encoding) comm.LDPCDecoder (decoding)
UFMC filter length	$N_{FFT}/32$
UFMC sub-band bandwidth	42
UFMC sub-band number	172
UFMC sub-band offset	484

1. Justification for the choice of CFO values

The normalized CFO values were varied from 0.01 to 0.05. The choice of a maximum CFO equal to 0.05 was justified as follows: The normalized CFO was computed assuming that the transmission frequency was the first DVB-T2 frequency, which is equal to 474 MHz. Indeed, the DTT frequency band varies from 470 MHz to 862 MHz [37]. However, the 790–862 MHz band, called first digital dividend, has been released from Digital Terrestrial Television (DTT) applications. Therefore, the frequency band varying from 470 MHz to 790 MHz is the one used by many countries for DTT deployment [38]. The frequency carrier within this range is equal to 474 MHz. The normalized CFO represents ϵ in Equation (6) [34]. This formula is more detailed in Equation (14). This value was gathered by first computing the Doppler shift, as this value depends on the Doppler shift and the OFDM symbol duration, and second, the CFO values. The Doppler shifts were computed using the simulation parameters for the mobile speeds of 50 km/h and 150 km/h. The absolute value of the Doppler shift was computed using Equations (15) and (16) for each value of mobile speed.

$$\Delta f_{D_{Max}} = \frac{50}{3.6} \times \frac{474 \times 10^6}{3 \times 10^8} = 21.94Hz \quad (15)$$

$$\Delta f_{D_{Max}} = \frac{150}{3.6} \times \frac{474 \times 10^6}{3 \times 10^8} = 65.83Hz \quad (16)$$

$\Delta f_{D_{Max}}$ values are equal to 21.94 Hz and 65.83 Hz for the mobile speeds of 50 km/h and 150 km/h, respectively.

Moreover, the OFDM simulation parameters such as the number of subcarriers $N_{FFT} = 8192$ and the channel bandwidth $B = 8$ MHz were exploited to compute the subcarrier spacing f_1 using Equations (9) and (10). The subcarrier spacing was then equal to 1116.07 Hz, as computed in Equation (18).

$$f_1 = \frac{\frac{64}{7} \times \frac{B}{8}}{N_{FFT}} \tag{17}$$

$$f_1 = \frac{\frac{64}{7} \times \frac{8\times10^6}{8}}{8192} = 1116.07 Hz \tag{18}$$

The OFDM symbol duration was equal to the inverse of the subcarrier spacing as already mentioned in Equation (8). The OFDM symbol duration was then equal to 896 µs. Therefore, the normalized CFO value was computed using Equations (6) and (14).

- For a vehicle speed of 50 km/h, the Doppler shift was equal to 21.94 Hz, and the normalized CFO was equal to 0.0197
- For a vehicle speed of 150 km/h, the Doppler shift was equal to 65.83 Hz, and the normalized CFO was equal to 0.0590

These values were used for the simulation, considering an approximation to two decimal places where CFO varied from 0.01 to 0.05.

2. Justification for the choice of other parameters values

DVB-T2 defines five channel bandwidths: 1.7 MHz, 6 MHz, 7 MHz, 8 MHz, and 10 MHz. The channel bandwidth of 8 MHz was chosen as it is the most used in DTT deployment. In particular, the DVB consortium defined a spreadsheet which contained a set of configuration parameters useful for broadcasters during deployment [39]. All of these configurations only included a channel bandwidth of 8 MHz.

DVB-T2 defines six numbers of subcarriers: 1024 (1K mode), 2048 (2K mode), 4096 (4K mode), 8192 (8K mode), 16,384 (16K mode), and 32,768 (32K mode). K is equal to 1024 subcarriers. As defined in [35] (pages 846–847), the higher the number of subcarriers, the closer the subcarriers are to each other, and the more sensitive DVB-T2 is to the Doppler effect. Then, low numbers of subcarriers are recommended for mobile reception in DVB-T2. Furthermore, mobile reception was tested in some countries where the last three modes' performance was analyzed by field measurements. It was demonstrated that the 8K mode presented higher performance than the 16K mode, which in turn had higher performance than the 32K mode [35] (pages 846–847). It was noted that the 32K mode was worse for mobile reception with a mobile speed varying from 60 km/h to 100 km/h. Therefore, the choice was made to use the 8K mode (8192 subcarriers), to see the impact on the simulation of the increase in CFO and consequent increase in mobile speed to 150 km/h.

DVB-T2 defines four constellation orders: 4-QAM, 16-QAM, 64-QAM, and 256-QAM. As the constellation order increases, so does the number of bits transmitted per symbol. As a result, throughput increases. But higher-order QAMs such as 64-QAM and 256-QAM are more susceptible to noise and interference because the constellation points are closer together. As the purpose of this study was to evaluate the robustness of DVB-T2 signals, the choice was made to use 16-QAM, which is more robust and reliable in difficult environmental conditions. It is relevant to note that 4-QAM is the most robust QAM. However, it is the constellation order with the lowest bit rate.

LDPC is the Forward Error Correction (FEC) code used in DVB-T2, Digital Video Broadcasting Satellite, second generation (DVB-S2), and ATSC 3.0 which allows these systems to be closer to the Shannon limit. Compared to convolutional codes used in DVB-T, LDPC codes are block codes designed to transmit information over a noisy channel. These codes are represented using sparse bipartite graphs, in which nodes constitute code bits and parity-check equations. The sparseness of the graph allows one to perform an efficient decoding. The main peculiarity of these codes is the decoding process, which is performed using a Tanner graph and an iterative decoding algorithm. The algorithm used to process the decoding is a soft iterative decoding called "Belief Propagation" algorithm [40]. In DVB-T2, the parity check equations are used to construct the control parity check matrix used during the encoding process and the decoding process. As Matlab was the simulation tool used for our simulation, the main function used for LDPC were **dvbs2ldpc**, which allowed us to construct the control parity check matrix, and **comm.LDPCEncoder** and **comm.LDPCDecoder**, for the encoding and the decoding process [41]. The control parity check matrix was constructed by considering the code rate to exploit for encoding and decoding. It is important to note that the last two Matlab functions were replaced by **ldpcencode** and **ldpcdecode**, respectively, from Matlab version R2021b to the current version. Six code rates are defined in DVB-T2. There are 1/2, 3/5, 2/3, 3/4, 4/5, 5/6. The 1/2 code was used in our simulation as it was the code rate that offered the highest signal robustness.

As previously presented in Section 3.1.2, UFMC configuration requires four parameters: the filter length, the sub-band bandwidth, the sub-band number, and the sub-band offset. As a comparison was performed with OFDM, the filter length should cover the number of samples used for the cyclic prefix in OFDM. In the conventional UFMC, the filter length is equal to the cyclic prefix length [42]. In our simulation case, the CP was equal to 1/32, which corresponded to a cyclic prefix length of $N_{FFT}/32 = 8192/32 = 256$. Therefore, the UFMC filter length was equal to 256. Once the filter length was identified, the other parameter values were chosen on the basis that parameters followed Equation (19).

$$N_{NFFT} = (sub - bandbandwidth \times sub - bandnumber) + (2 \times Sub - bandoffset) \quad (19)$$

Furthermore, as the CP is not used in UFMC, this latter implies an increase in spectral efficiency in comparison with OFDM. The spectral efficiency of UFMC was compared to the 100% OFDM spectral efficiency using Equation (20), previously presented in [9]. This value is expressed as a percentage. That equation computes the overhead percentage spared when UFMC is used instead of OFDM. M_{OFDM} is the number of data subcarriers used in OFDM, M_{UFMC} is the number of data subcarriers used in UFMC, and N_{FFT} is the total number of subcarriers

$$P_{Overhead-OFDM-UFMC} = 100 \times (1 - \frac{M_{OFDM}}{M_{UFMC} + (N_{FFT} \times CP)}) \quad (20)$$

In the case of the DVB-T2 parameters used, that is, an 8K mode, i.e., 8192 subcarriers, and a CP of 1/32, the UFMC was 103.03% spectrally efficient compared to the 100% OFDM if only the overhead induced by the CP was considered. The UFMC was 108.86% spectrally efficient compared to OFDM when the overhead induced by both the guard band and the CP were considered.

4.3. Figures of Merit

The performance parameters used as figures of merit in our simulations were the BER, Signal to Noise Ratio (SNR), MER, and EVM.

- The BER is defined as the ratio of the number of erroneous bits to the number of transmitted bits within a period. The lower the number of erroneous bits, the better the system performance. In this work, the BER was computed after the constellation demapping and LDPC decoder.
- The SNR is described as the fraction of the received signal strength over the noise strength within the frequency bandwidth range of operation. It measures the quality of the signal relative to the background noise.
- The MER is viewed as an indicator of the modulation quality of the received signal. Defined in [43], this metric measures the QAM symbols' accuracy. A high MER value means good signal quality. The MER is approximately equal to the SNR when only

white Gaussian noise is present in the signal. The EVM is a parameter also presented in [43]; the lower its value, the better the system's performance.

5. Results

In this section, simulation results are presented for OFDM and UFMC case studies in DVB-T2 using BER, MER, and EVM performance evaluation metrics.

5.1. Performance Evaluation of DVB-T2 Using BER

5.1.1. Native DVB-T2 Without LDPC Coder

In this part, the CFO impact on the native DVB-T2 system is shown when a fading channel is used or not.

Figure 12 shows the BER evolution as a function of the SNR in the native DVB-T2 when only Gaussian noise was used for various CFO values. One can note that when the CFO was not applied (CFO = 0.00), the SNR value was equal to 18.4 dB at a BER of 10^{-4}. At a SNR value of 20 dB, the BER values of 5.4×10^{-6}, 1.2×10^{-5}, 10^{-4}, 8.3×10^{-4}, 4.2×10^{-3}, and 1.4×10^{-2} were obtained for CFO values of 0, 0.01, 0.02, 0.03, 0.04, and 0.05, respectively. These results show that the system performance decreased in the presence of an increasing CFO and the penalty obtained increased with the CFO values. At a BER of 10^{-2}, the loss gathered varied from 0.2 dB to 7.8 dB. The main reason for the signal performance degradation was the ICI induced by the CFO on the noisy signal. This ICI was noticed by the offset in the OFDM subcarriers. This offset was materialized by the degradation of the symbols carried by these subcarriers.

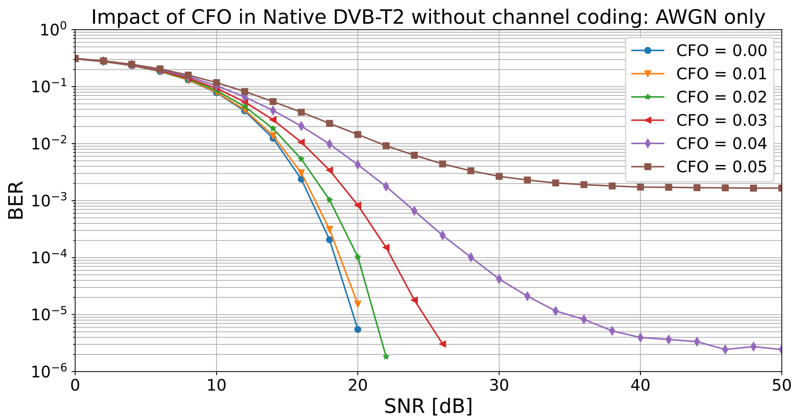

Figure 12. BER versus SNR in the native DVB-T2 system without coding: CFO impact evaluation in the AWGN case.

Figure 13 presents the BER evolution as a function of the SNR in the native DVB-T2 when a TU6 channel and Gaussian noise were used for various CFO values. It is remarkable that when the CFO was not applied, the SNR value equaled 42 dB at a BER of 10^{-4}. This value (42 dB instead of 18.4 dB) shows the TU6 channel's impact compared to the simulation results of Figure 12. In other words, the TU6 channel caused a loss of 23.6 dB on the system performance. Also, at the SNR value of 40 dB, the BER values of 1.5×10^{-4}, 1.6×10^{-4}, 2.1×10^{-4}, 3.3×10^{-4}, 4.8×10^{-4}, and 2.6×10^{-3} were obtained for CFO values of 0, 0.01, 0.02, 0.03, 0.04, and 0.05, respectively. One can note the performance degradation with the CFO values increase when the TU6 channel was used. At a BER of 10^{-2}, the loss induced by the CFO varied up to 6 dB, depending on the CFO value. The increase in BER degradation was due to the "multipath" nature of the channel, which added a time dispersion between symbols (ISI) to the frequency dispersion due to the CFO (ICI). The trends observed in our simulation results are in line with the theoretical models developed in [44].

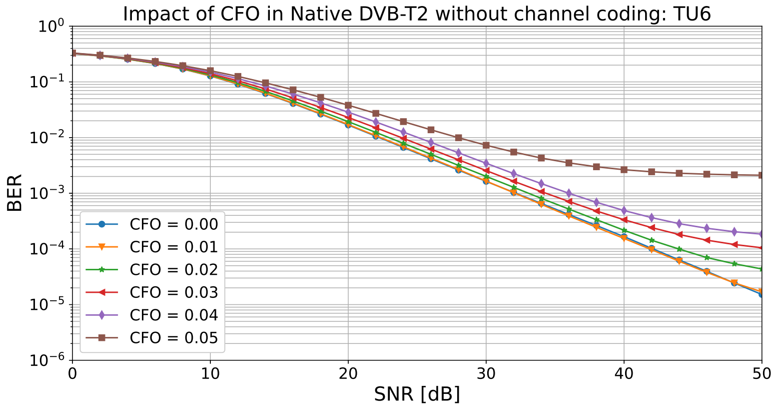

Figure 13. BER versus SNR in the native DVB-T2 system without coding: CFO evaluation in the TU6 and AWGN case.

5.1.2. UFMC-Based DVB-T2 Without LDPC Coder

In this part, the CFO impact is shown in the UFMC-based DVB-T2 system (cf. Figure 11) when a fading channel is used or not.

Figure 14 exhibits the BER evolution as a function of the SNR in the UFMC-based DVB-T2 when only Gaussian noise was used for various CFO values. One can note that when the CFO was not applied, the SNR value was equal to 18.4 dB at a BER of 10^{-4}. This result allows us to conclude that UFMC-based DVB-T2 and the native DVB-T2 present the same performance in the presence of Gaussian noise only. Furthermore, at a SNR value of 20 dB, the BER values of 3.1×10^{-5}, 5.6×10^{-5}, 1.9×10^{-4}, 8.2×10^{-4}, 3.2×10^{-3}, and 10^{-2} were obtained for CFO values 0, 0.01, 0.02, 0.03, 0.04, and 0.05, respectively. One can note that the loss increased with the CFO value. However, the loss induced by the CFO values of 0.04 and 0.05 with UFMC-based DVB-T2 were lower than those induced by the CFO values of 0.04 and 0.05 with the native DVB-T2 system. At a BER of 10^{-2}, the loss induced by the CFO varied from 0.1 dB to 6 dB in the UFMC-based DVB-T2 case. In other words, the loss induced by CFO values of 0.04 and 0.05 in UFMC-based DVB-T2 system were 3 dB and 6 dB, respectively, at a BER of 10^{-2}, when the SNR values were compared to those obtained without CFO. In contrast, the losses induced by CFO values of 0.04 and 0.05 in the native DVB-T2 system were 3.8 dB and 7.8 dB, respectively, at a BER of 10^{-2}. Thus, we can conclude that the impact of the CFO is more noticeable with OFDM waveforms than UFMC waveforms. UFMC is less sensitive to the CFO than OFDM in the AWGN-only case, as highlighted in [27], which presents the SER versus SNR UFMC performance compared with the OFDM performance.

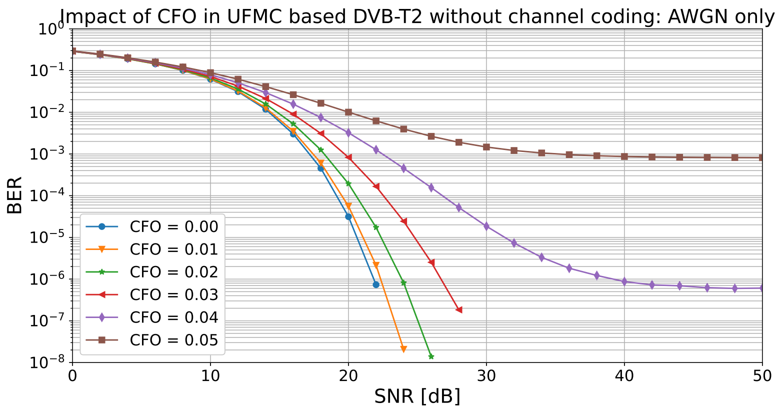

Figure 14. BER versus SNR in the UFMC-based DVB-T2 system without coding: CFO evaluation in the AWGN-only case.

Figure 15 shows the BER evolution as a function of the SNR in the UFMC-based DVB-T2 when the TU6 channel was used. By comparing the UFMC-based DVB-T2 system performance to the native DVB-T2 system performance in the TU6 case in Figure 13, one can find that UFMC presented better performance than OFDM when the TU6 fading channel was used. When the CFO was not applied, at the same BER of 10^{-4}, the SNR value of UFMC-based DVB-T2 was equal to 32 dB instead of 42 dB in the native DVB-T2 system. Furthermore, this figure demonstrates that UFMC performance slowly degrades with the increase in the CFO value. The system performance without CFO was approximately equal to the system performance when the CFO value varied from 0.01 to 0.04. For a CFO value of 0.05, the system performance decreased, and the loss induced was equal to 14 dB at a BER of 10^{-3}. One can conclude that UFMC is less sensitive to the CFO than OFDM in the presence of a TU6 channel when the coding technique is not implemented in the system, as the induced losses are less than those for OFDM, which represents the same trend as when only adding AWGN.

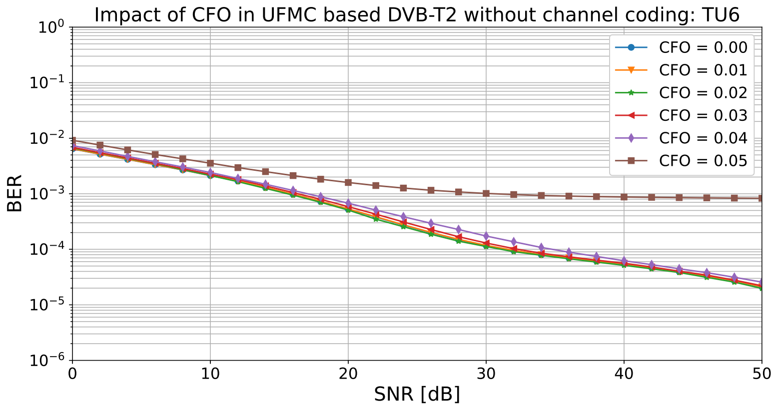

Figure 15. BER versus SNR in the UFMC-based DVB-T2 system without coding: CFO evaluation in the TU6 and AWGN case.

Table 4 presents a summary of the performance of OFDM and UFMC in the presence of a CFO when AWGN is the only impairment considered and when TU6 channel is additionally used.

Table 4. Native DVB-T2 (OFDM) and UFMC-based DVB-T2 performance without LDPC coding and with CFO.

AWGN Case (SNR = 20 dB)			AWGN and TU6 Channel Case (SNR = 40 dB)		
CFO	**OFDM BER**	**UFMC BER**	**CFO**	**OFDM BER**	**UFMC BER**
0.00	5.4×10^{-6}	3.1×10^{-5}	0.00	1.5×10^{-4}	6.0×10^{-5}
0.01	1.2×10^{-5}	5.6×10^{-5}	0.01	1.6×10^{-4}	6.0×10^{-5}
0.02	1.2×10^{-4}	1.9×10^{-4}	0.02	2.1×10^{-4}	6.0×10^{-5}
0.03	8.3×10^{-4}	8.2×10^{-4}	0.03	3.3×10^{-4}	6.0×10^{-5}
0.04	4.2×10^{-3}	3.2×10^{-3}	0.04	4.8×10^{-4}	7.0×10^{-5}
0.05	1.4×10^{-2}	1.0×10^{-2}	0.05	2.6×10^{-3}	9.0×10^{-4}

5.1.3. Native DVB-T2 with LDPC Coder

Previously, the CFO performance in DVB-T2 was evaluated when the coding channel was not applied. Here, LDPC coding was applied in the systems and the CFO performance was evaluated.

Figure 16 gives the results from the BER simulation versus SNR. First, one can note that a BER of 10^{-5} was obtained at the SNR value of 6.18 dB for a CFO value of 0.00. These results allow us to conclude that the simulator behaves well as highlighted in the DVB-T2 implementation guidelines [45]. Moreover, the system performance diminished when CFO was considered, and this reduction was more prominent with the increase in CFO. At a BER value of 10^{-5}, the SNR values of 6.18 dB, 6.23 dB, 6.28 dB, 6.74 dB, and 7.14 dB were identified for CFO values 0, 0.01, 0.02, 0.04, and 0.05, respectively. This result means that the losses induced by the different CFO values were 0.05 dB, 0.1 dB, 0.56 dB, and 0.96 dB for CFO values 0.01, 0.02, 0.04, and 0.05, respectively.

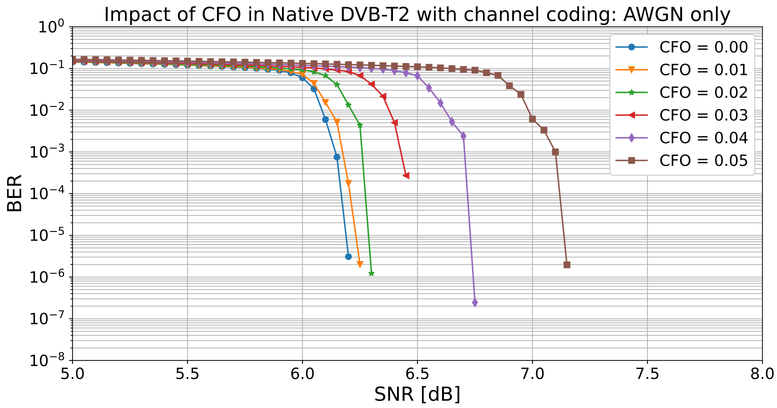

Figure 16. BER versus SNR in the native DVB-T2 system with coding: CFO evaluation in the AWGN-only case.

Figure 17 highlights the BER evolution as a function of SNR when the TU6 channel and channel coding were applied in the native DVB-T2 system. A slow BER decrease was noticed in the SNR range 0–10 dB, a rapid BER improvement in the SNR range 10–16 dB, and a BER stability after 16 dB. This behavior of the BER can be justified by the presence of LDPC iterative decoding (whose BER performance presents three regions such as the no-convergence region, the waterfall region, and the error-floor region [46]). While the waterfall region was a region of quick decrease in the BER, the error-floor region appeared at a low BER and was characterized by a very slow decrease in the BER. Furthermore, it was noted a low BER performance decrease with the CFO augmentation. At a BER of 10^{-2}, the losses induced by the CFO insertion varied from 0.5 dB to 0.8 dB. At a BER of 2×10^{-3}, the losses induced by the CFO insertion varied from 0.1 dB to 0.6 dB. One can conclude that when coding channel is applied, the CFO impact is not highly noticeable in the presence of the TU6 channel in comparison with the AWGN-only channel.

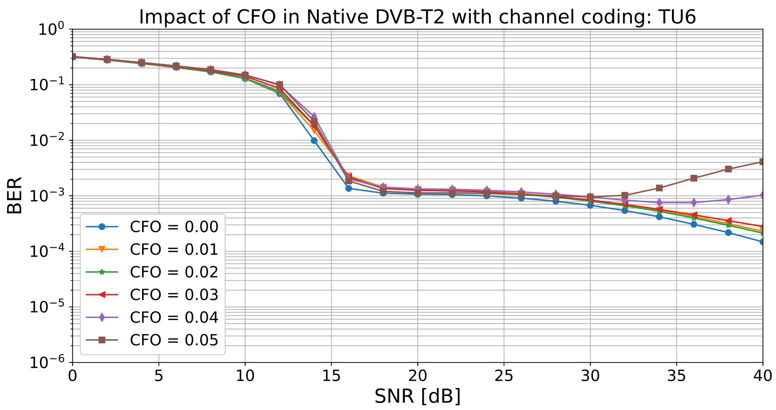

Figure 17. BER versus SNR in the native DVB-T2 system with coding: CFO evaluation in the TU6 and AWGN case.

5.1.4. NUC-Based DVB-T2 with LDPC Coder

Previously, the native DVB-T2 system performance with LDPC was presented when only Gaussian noise was considered and also when a TU6 channel was considered. Here, we show NUCs' performance in DVB-T2 and the CFO impact in the NUC-based DVB-T2 system in both AWGN and TU6 cases.

Figure 18 gives a view of the results gathered with only Gaussian noise. The SNR values of 6.02 and 6.04 were obtained at a BER of 10^{-4} and 10^{-5}, respectively. By comparing those values to those obtained in the native DVB-T2 case without CFO (Figure 16), we can conclude that the 2D-NUCs allowed gains of 0.15 dB and 0.14 dB at a BER of 10^{-4} and 10^{-5}, respectively. Additionally, when a CFO was applied in that system, it engendered losses of 0.04 dB, 0.11 dB, 0.25 dB, and 0.54 dB at a BER of 10^{-4} for CFO values of 0.01, 0.02, 0.03, and 0.04, respectively. This loss increased up to 0.85 dB for 0.05 CFO value. By comparing the maximum CFO loss to that obtained with the native DVB-T2 (Figure 16), one can conclude that the difference was 0.011 dB and the losses of both systems (native DVB-T2 and 2D-NUC-based) were under 0.1 dB.

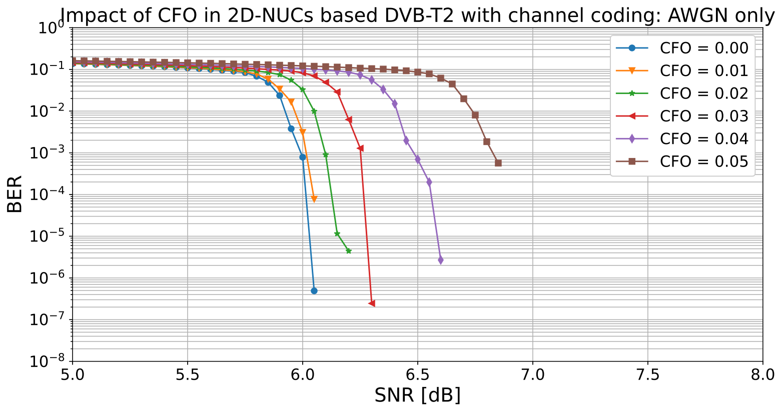

Figure 18. BER versus SNR in the NUC-based DVB-T2 system with coding: CFO evaluation in the AWGN-only case.

Figure 19 illustrates the BER performance as a function of SNR when QAM was substituted for NUCs in the DVB-T2 system using a TU6 channel instead of only Gaussian noise. The same behavior of BER curves as in Figure 17 is demonstrated here. These results mean that the CFO performance losses of NUC-based DVB-T2 were comparable to those obtained with the native DVB-T2 using TU6 channel.

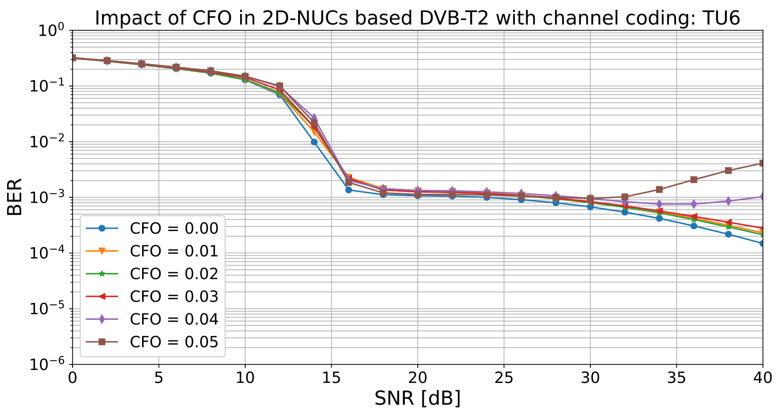

Figure 19. BER versus SNR in the NUC-based DVB-T2 system with coding: CFO evaluation in the TU6 and AWGN case.

5.1.5. UFMC-Based DVB-T2 with LDPC Coder

As we have already shown the results about the CFO impact on the coded DVB-T2 system, the results about the UFMC insertion in DVB-T2 are presented below.

Figure 20 exposes the BER versus SNR performance when OFDM was substituted by UFMC in the native DVB-T2 coded system. It was observed that the UFMC DVB-T2 system performance without CFO was 0.1 dB lower than the native DVB-T2 system performance without CFO at a BER of 10^{-3}. Additionally, at that BER value, the SNR values of 6.33 dB, 6.39 dB, 6.45 dB, 6.59 dB, 6.87 dB, and 7.25 dB were identified for CFO values 0, 0.01, 0.02, 0.03, 0.04, and 0.05, respectively. At a BER value of 10^{-5}, the SNR value was 7.27 dB for CFO = 0.05. The losses induced by the CFO varied from 0.06 to 0.94 dB. In a nutshell, the CFO impact on the native DVB-T2 system was comparable to that viewed in the UFMC-based DVB-T2 system when the coding technique was applied.

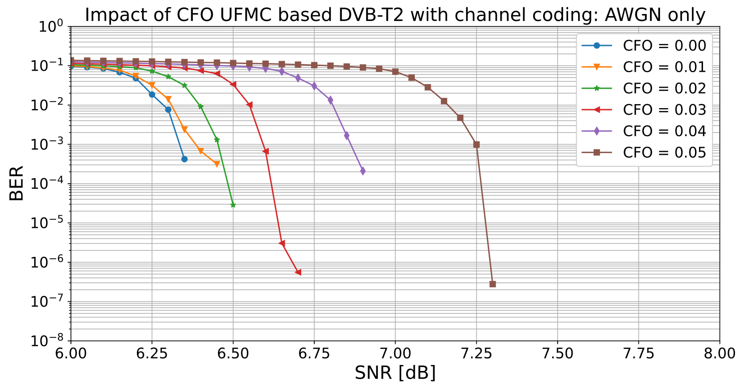

Figure 20. BER versus SNR in the UFMC-based DVB-T2 system with coding: CFO evaluation in the AWGN-only case.

Figure 21 exhibits the BER evolution as a function of SNR for the UFMC-based DVB-T2 system when the LDPC coding technique was applied. The impact of the TU6 channel on UFMC performance is shown. When CFO was not considered, at BER values of 10^{-3} and 10^{-4}, the SNR values were equal to 9 dB and 13 dB, respectively. This result means that the TU6 channel induced a loss of 2.67 dB for a BER of 10^{-3} when UFMC was used instead of OFDM. In contrast, a TU6 channel loss of 9.87 dB was obtained at a BER of 10^{-3}, as seen when comparing Figure 17 to Figure 16. This result allows us to conclude that the UFMC performance is better than the OFDM performance in the DVB-T2 system in the presence of the TU6 channel. Moreover, when CFO was applied in UFMC-based DVB-T2 using the TU6 channel, the losses induced by the CFO increase were negligible for CFO values of 0.01, 0.02, and 0.03. That loss was equal to 0.2 dB at BER values of 10^{-3} and 10^{-4} for the CFO value of 0.05. Then, we can conclude that the CFO impact on the UFMC-based DVB-T2 system is lower than that with the native DVB-T2.

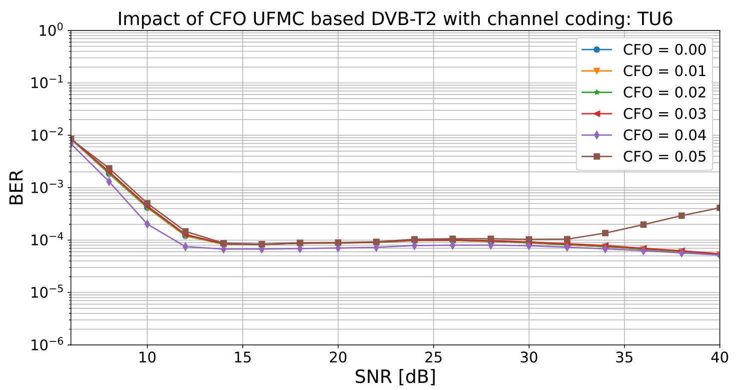

Figure 21. BER versus SNR in the UFMC-based DVB-T2 system with coding: CFO evaluation in the TU6 and AWGN case.

5.1.6. UFMC-Based DVB-T2 with LDPC Coder and 2D-NUCs

Previously, QAM was substituted for 2D-NUCs (cf. Section 5.1.4) and OFDM was substituted for UFMC (cf. Section 5.1.5) in the DVB-T2 system. Their performance were independently estimated. In this part, the performance of NUCs and UFMC was jointly evaluated in the DVB-T2 system. In other words, QAM and OFDM were both substituted by 2D-NUCs and UFMC. The CFO was applied to check the induced losses on the system performance.

Figure 22 shows the CFO performance when UFMC and NUCs were used together in DVB-T2. It was observed that at a BER of 10^{-3}, the SNR value of this system without CFO was 6.2 dB with UFMC/NUCs whereas this value was equal to 6.33 dB with UFMC (Figure 20). This result permits us to conclude about the gain of 0.13 dB induced by 2D-NUCs in the UFMC-based DVB-T2 system. Moreover, at a BER of 10^{-3}, the losses caused by CFO were 0.08 dB, 0.15 dB, 0.3 dB, 0.52 dB, and 0.83 dB for CFO values of 0.01, 0.02, 0.03, 0.04, and 0.05, respectively. We can conclude that the CFO impact on both UFMC-based DVB-T2 and UFMC/NUC-based DVB-T2 is the same when only Gaussian noise is used.

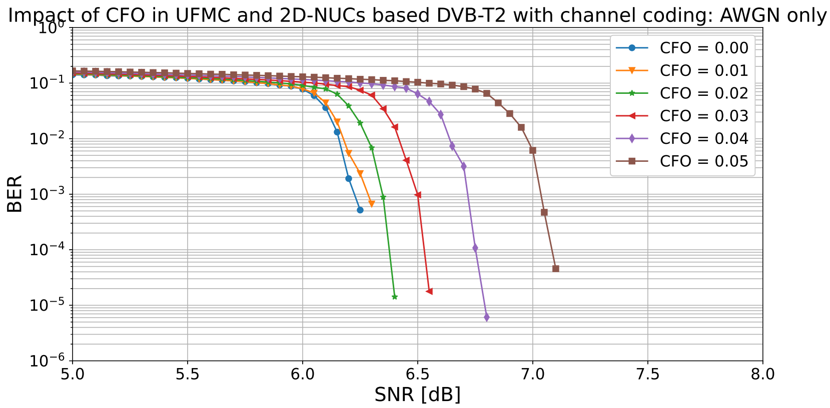

Figure 22. BER versus SNR in the UFMC/NUC-based DVB-T2 system with coding: CFO evaluation in the AWGN-only case. The comparison of curves in terms of signal-to-noise ratio (SNR) values obtained at different BER values (10^{-3}, 10^{-4}, 10^{-5}) is shown in the following table.

Figure 23 exposes the BER evolution as a function of the SNR when the TU6 channel was used. The CFO impact on the FBMC/NUC-based DVB-T2 system performance is highlighted. One can note that there was a negligible loss when the CFO was inserted in the system in comparison with the DVB-T2 native case (Figure 17) where the loss varied up to 1 dB, corresponding to a CFO value of 0.05.

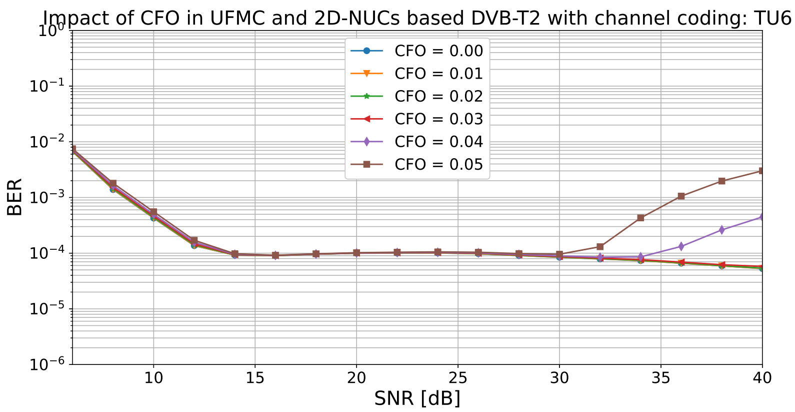

Figure 23. BER versus SNR in the UFMC/NUC-based DVB-T2 system with coding: CFO evaluation in the TU6 and AWGN case. The comparison of curves in terms of signal-to-noise ratio (SNR) values obtained at different BER values (10^{-3}, 10^{-4}, 10^{-5}) is shown in the following table.

In conclusion, the CFO impact decreased when LDPC coding was applied in the system. When the TU6 fading channel was used, the CFO losses were lower than those with Gaussian noise only in the native DVB-T2 system, UFMC-based DVB-T2, NUC-based DVB-T2, and UFMC/NUC-based DVB-T2. Furthermore, UFMC outperformed OFDM in the presence of a TU6 channel, and 2D-NUCs outperformed QAM in the presence of only Gaussian noise for the low-SNR region. For the high-SNR region (above 30 dB), we observed the system performance degradation for a CFO value of 0.05. In particular, when UFMC was applied in the system, this performance decrease was more noticeable above 30 dB when the CFO value increased. Table 5 presents the performance of native DVB-T2 (Figures 16 and 17) and NUC-based DVB-T2 (Figures 18 and 19) in the presence of a CFO. This table shows the performance of the systems (native DVB-T2 and NUC-based DVB-T2) when QAM in the native DVB-T2 system was substituted for NUCs. Table 6 presents the performance of native DVB-T2 (Figures 16 and 17) and UFMC based DVB-T2 (Figures 20 and 21) in the presence of a CFO. This table shows the performance of the systems (native DVB-T2 and UFMC based DVB-T2) when OFDM in the native DVB-T2 system was substituted for UFMC. Table 7 presents the performance of native DVB-T2 (Figures 16 and 17) and UFMC/NUC-based DVB-T2 (Figures 22 and 23) in the presence of a CFO. This table shows the performance of the systems (native DVB-T2 and UFMC/NUC-based DVB-T2) when QAM and OFDM in the native DVB-T2 system were substituted for NUCs and UFMC, respectively. Results are highlighted for the BER values of 10^{-3}, 10^{-4}, and 10^{-5} when only AWGN was considered and the BER values of 10^{-2}, 2×10^{-3}, and 10^{-3} when the TU6 channel and AWGN were considered.

Table 5. Native DVB-T2 (QAM) and NUC-based DVB-T2 performance with LDPC coding and with CFO—Reader's key: the second column gives the SNR values [dB] required to guarantee the three target bit error rates for native DVB-T2 subject to CFO values ranging from 0.00 to 0.05, respectively. The third column contains the same representation but for DVB-T2 using a non-uniform constellation. The fourth column represents the penalty in terms of SNR [dB] implied by each CFO value applied to native DVB-T2 (see column 4). Finally, the fifth column gives the same values, but in the case of DVB-T2 with a non-uniform constellation (see column 3).

QAM vs. NUCs: AWGN-only case for 3 different BERs (10^{-3}, 10^{-4}, 10^{-5})												
CFO	**Native DVB-T2 SNR [dB]**			**NUC-based DVB-T2 SNR [dB]**			**Native DVB-T2 CFO SNR penalties [dB]**			**NUC-based DVB-T2 CFO SNR penalties [dB]**		
ϵ	**BER** 10^{-3}	**BER** 10^{-4}	**BER** 10^{-5}	**BER** 10^{-3}	**BER** 10^{-4}	**BER** 10^{-5}	**BER** 10^{-3}	**BER** 10^{-4}	**BER** 10^{-5}	**BER** 10^{-3}	**BER** 10^{-4}	**BER** 10^{-5}
0.00	6.14	6.16	6.18	5.98	6.01	6.04	–	–	–	–	–	–
0.01	6.18	6.21	6.23	6.02	6.05	–	0.04	0.05	0.05	0.04	0.04	–
0.02	6.26	6.27	6.28	6.10	6.12	6.15	0.12	0.11	0.10	0.12	0.11	0.11
0.03	6.43	–	–	6.25	6.26	6.28	0.29	–	–	0.27	0.25	0.24
0.04	6.70	6.71	6.74	6.47	6.55	6.58	0.56	0.55	0.56	0.49	0.54	0.54
0.05	7.10	7.11	7.14	6.82	–	–	0.96	0.95	0.96	0.84	–	–
QAM vs. NUCs: AWGN and TU6 channel case for 3 different BERs (10^{-2}, 2.10^{-3}, 10^{-3})												
CFO	**Native DVB-T2 SNR [dB]**			**NUC-based DVB-T2 SNR [dB]**			**Native DVB-T2 CFO SNR penalties [dB]**			**NUC-based DVB-T2 CFO SNR penalties [dB]**		
ϵ	**BER** 10^{-2}	**BER** 2.10^{-3}	**BER** 10^{-3}	**BER** 10^{-2}	**BER** 2.10^{-3}	**BER** 10^{-3}	**BER** 10^{-2}	**BER** 2.10^{-3}	**BER** 10^{-3}	**BER** 10^{-2}	**BER** 2.10^{-3}	**BER** 10^{-3}
0.00	14.0	15.5	23.5	14	15.5	23.5	–	–	–	–	–	–
0.01	14.5	16.1	27.5	14.5	16.1	27.5	0.5	0.6	4.0	0.5	0.6	4.0
0.02	14.5	16.0	27.5	14.5	16.0	27.5	0.5	0.5	4.0	0.5	0.5	4.0
0.03	14.7	16.0	27.5	14.7	16.0	27.5	0.7	0.5	4.0	0.7	0.5	4.0
0.04	14.7	16.0	28.0	14.7	16.0	28.0	0.7	0.5	4.5	0.7	0.5	4.5
0.05	14.8	16.0	27.5	14.8	16.0	27.5	0.8	0.5	4.0	0.8	0.5	4.0

Table 6. Native DVB-T2 (OFDM) and UFMC-based DVB-T2 performance with LDPC coding and with CFO—Similar reader's key as in Table 5.

OFDM vs. UFMC: AWGN case only for 3 different BERs (10^{-3}, 10^{-4}, 10^{-5})												
CFO	**Native DVB-T2 SNR [dB]**			**UFMC-based DVB-T2 SNR [dB]**			**Native DVB-T2 CFO SNR penalties [dB]**			**UFMC-based DVB-T2 CFO SNR penalties [dB]**		
ϵ	**BER** 10^{-3}	**BER** 10^{-4}	**BER** 10^{-5}	**BER** 10^{-3}	**BER** 10^{-4}	**BER** 10^{-5}	**BER** 10^{-3}	**BER** 10^{-4}	**BER** 10^{-5}	**BER** 10^{-3}	**BER** 10^{-4}	**BER** 10^{-5}
0.00	6.14	6.16	6.18	6.33	–	–	–	–	–	–	–	–
0.01	6.18	6.21	6.23	6.39	–	–	0.04	0.05	0.05	0.06	–	–
0.02	6.26	6.27	6.28	6.45	6.48	–	0.12	0.11	0.10	0.12	–	–
0.03	6.43	–	–	6.59	6.63	6.65	0.29	–	–	0.26	–	–
0.04	6.70	6.71	6.74	6.87	–	–	0.56	0.55	0.56	0.54	–	–
0.05	7.10	7.11	7.14	7.25	7.26	7.27	0.96	0.95	0.96	0.92	–	–
OFDM vs. UFMC: AWGN and TU6 channel case for 3 different BERs (10^{-2}, 2.10^{-3}, 10^{-3})												
CFO	**Native DVB-T2 SNR [dB]**			**UFMC-based DVB-T2 SNR [dB]**			**Native DVB-T2 CFO SNR penalties [dB]**			**UFMC-based DVB-T2 CFO SNR penalties [dB]**		
ϵ	**BER** 10^{-2}	**BER** 2.10^{-3}	**BER** 10^{-3}	**BER** 10^{-2}	**BER** 2.10^{-3}	**BER** 10^{-3}	**BER** 10^{-2}	**BER** 2.10^{-3}	**BER** 10^{-3}	**BER** 10^{-2}	**BER** 2.10^{-3}	**BER** 10^{-3}
0.00	14.0	15.5	23.5	–	7.5	8.5	–	–	–	–	–	–
0.01	14.5	16.1	27.5	–	7.5	8.5	0.5	0.6	4.0	–	0.0	0.0
0.02	14.5	16.0	27.5	–	7.5	8.5	0.5	0.5	4.0	–	0.0	0.0
0.03	14.7	16.0	27.5	–	7.5	8.5	0.7	0.5	4.0	–	0.0	0.0
0.04	14.7	16.0	28.0	–	–	–	0.7	0.5	4.5	–	–	–
0.05	14.8	16.0	27.5	–	7.7	8.7	0.8	0.5	4.0	–	0.2	0.2

5.2. Performance Evaluation of DVB-T2 Using MER and EVM

In this section, the MER and EVM performance values are shown for the DVB-T2 system.

5.2.1. Native DVB-T2 with LDPC Coder Using MER

As explained in Section 4.3, the MER gives an overview of the modulated signal quality. We present in this part the CFO performance using the MER instead of the BER as previously shown.

Figure 24 presents the MER evolution as a function of SNR. It is observed that when only Gaussian noise was applied, the MER was equal to the SNR without the presence of a CFO. In the presence of a CFO, the MER performance decreased with the increase in CFO value. In other words, the MER was lower than the SNR value for each CFO value. This result confirmed the BER evolution behavior and demonstrated that in the presence of CFO, above 30 dB, the MER did not increase even if the SNR increased.

Figure 25 exposes the CFO impact on the DVB-T2 system using the MER when the TU6 channel was applied. One can note the impact of the TU6 channel on the MER performance. Instead of having the MER equal to SNR as in the AWGN case without CFO, the MER was lower than the SNR when the CFO was not considered. At the SNR of 20 dB, the MER was equal to 10 dB, meaning that the TU6 channel induced a loss of 10 dB on the MER performance. Furthermore, when the CFO was applied, the MER performance decreased by up to 16 dB in comparison with the MER curve without CFO.

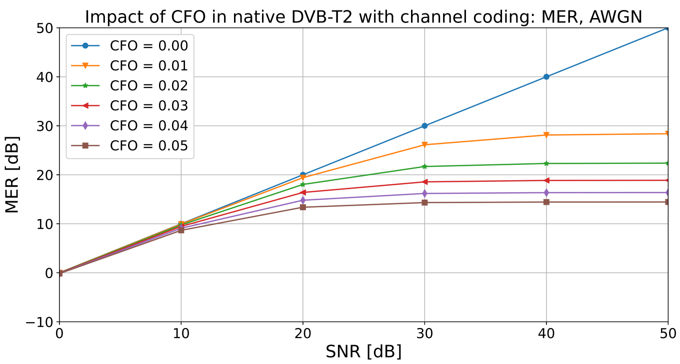

Figure 24. MER versus SNR in the native DVB-T2 system with coding: CFO evaluation in the AWGN-only case.

Table 7. Native DVB-T2 (OFDM) and UFMC/NUC-based DVB-T2 performance with LDPC coding and with CFO—Similar reader's key as in Table 5.

OFDM vs. UFMC/NUCs: AWGN case only for 3 different BERs (10^{-3}, 10^{-4}, 10^{-5})												
CFO	**Native DVB-T2 SNR [dB]**			**UFMC/NUC-based DVB-T2 SNR [dB]**			**Native DVB-T2 CFO SNR penalties [dB]**			**UFMC/NUC-based DVB-T2 CFO SNR penalties [dB]**		
ϵ	**BER** 10^{-3}	**BER** 10^{-4}	**BER** 10^{-5}	**BER** 10^{-3}	**BER** 10^{-4}	**BER** 10^{-5}	**BER** 10^{-3}	**BER** 10^{-4}	**BER** 10^{-5}	**BER** 10^{-3}	**BER** 10^{-4}	**BER** 10^{-5}
0.00	6.14	6.16	6.18	6.20	–	–	–	–	–	–	–	–
0.01	6.18	6.21	6.23	6.28	–	–	0.04	0.05	0.05	0.08	–	–
0.02	6.26	6.27	6.28	6.35	6.38	–	0.12	0.11	0.10	0.15	–	–
0.03	6.43	–	–	6.59	6.53	–	0.29	–	–	0.39	–	–
0.04	6.70	6.71	6.74	6.72	6.75	6.78	0.56	0.55	0.56	0.52	–	–
0.05	7.10	7.11	7.14	7.04	7.09	–	0.96	0.95	0.96	0.84	–	–
OFDM vs. UFMC/NUCs: AWGN and TU6 case for 3 different BERs (10^{-2}, 2.10^{-3}, 10^{-3})												
CFO	**Native DVB-T2 SNR [dB]**			**UFMC/NUC-based DVB-T2 SNR [dB]**			**Native DVB-T2 CFO SNR penalties [dB]**			**UFMC/NUC-based DVB-T2 CFO SNR penalties [dB]**		
ϵ	**BER** 10^{-2}	**BER** 2.10^{-3}	**BER** 10^{-3}	**BER** 10^{-2}	**BER** 2.10^{-3}	**BER** 10^{-3}	**BER** 10^{-2}	**BER** 2.10^{-3}	**BER** 10^{-3}	**BER** 10^{-2}	**BER** 2.10^{-3}	**BER** 10^{-3}
0.00	14.0	15.5	23.5	–	7.5	8.5	–	–	–	–	–	–
0.01	14.5	16.1	27.5	–	7.5	8.5	0.5	0.6	4.0	–	0.0	0.0
0.02	14.5	16.0	27.5	–	7.6	8.5	0.5	0.5	4.0	–	0.1	0.0
0.03	14.7	16.0	27.5	–	7.6	8.6	0.7	0.5	4.0	–	0.1	0.1
0.04	14.7	16.0	28.0	–	7.7	8.6	0.7	0.5	4.5	–	0.2	0.1
0.05	14.8	16.0	27.5	–	7.7	8.7	0.8	0.5	4.0	–	0.2	0.2

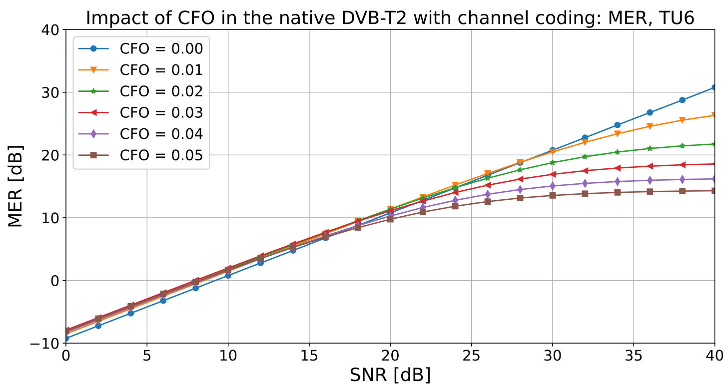

Figure 25. MER versus SNR in the native DVB-T2 system with coding: CFO evaluation in the TU6 and AWGN case.

5.2.2. Native DVB-T2 with LDPC Coder Using EVM

The CFO was evaluated using EVM when only Gaussian noise was applied and also with a TU6 channel.

Figure 26 presents the EVM evolution as a function of the SNR in the presence of only Gaussian noise. At the SNR value of 10 dB, the EVM value was equal to −10 dB. This behavior confirmed that the EVM was inversely proportional to the MER and SNR when the imperfection included in the signal was only Gaussian noise (cf. Figure 24).

Figure 27 presents the EVM evolution as a function of the SNR in the presence of a TU6 channel. At the SNR values of 10 dB and 20 dB, the EVM values were equal to 0 dB and −10 dB. This behavior showed the impact of the TU6 channel already highlighted with the MER performance. This result confirmed the proportionality of EVM to MER, which also occurred when a CFO was applied to this communication system. Furthermore, when the CFO was considered in the system, EVM values obtained were inversely proportional to the MER values obtained with the various CFOs.

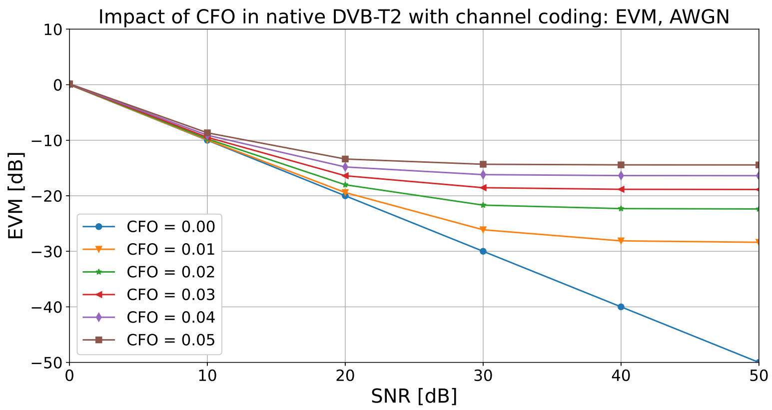

Figure 26. EVM versus SNR in the native DVB-T2 system with coding: CFO evaluation in AWGN case only.

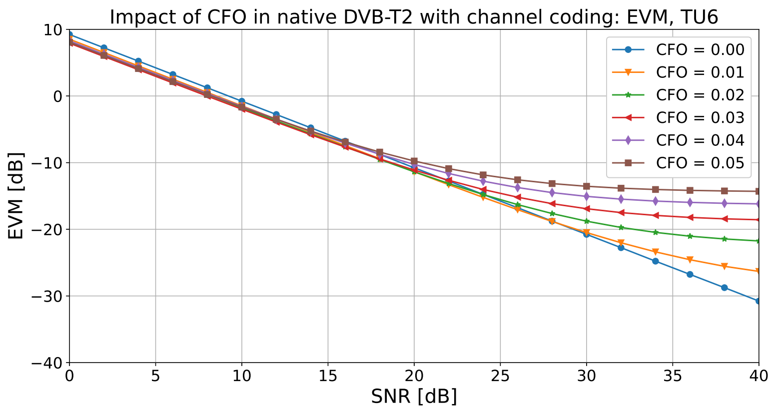

Figure 27. EVM versus SNR in the native DVB-T2 system with coding: CFO evaluation in the TU6 and AWGN case.

6. Discussion

In a nutshell, the CFO impact was evaluated in the framework of the DVB-T2 system using three performance evaluation tools: the BER, MER, and EVM. Moreover, the CFO impact was studied when advanced modulation schemes like NUCs and UFMC were applied in the native DVB-T2 system. The CFO values were varied from 0.01 to 0.05. It was demonstrated that the BER of the DVB-T2 system quickly increased with the CFO increase. The main conclusions from the results analysis are summarized as follows.

Firstly, the higher the velocity of the mobile, the greater the value of the Doppler shift, and the greater the value of the normalized CFO. This value has an impact on the increase in terms of ICI. This becomes more noticeable as the number of subcarriers increases, because the greater the number of subcarriers, the smaller the intercarrier spacing. In our simulations, we used 8192 subcarriers. If we had to increase this number to 32,768, the impact of the CFO would be more considerable. Indeed, the subcarrier spacing used for the case of 32,768 subcarriers is the subcarrier spacing value for 8192 subcarriers divided by four. It is then equal to 279 Hz. This value is not large enough compared to the Doppler shift values. Thus, the impact of ICI should really be noticeable on the OFDM signal.

Secondly, the lower the carrier frequency, the lower the Doppler shift value, and the lower the normalized CFO value. This means that using high transmission frequencies to transmit audiovisual signals, combined with a high number of subcarriers, could be more challenging for broadcasters when broadcasting signals to mobile receivers. DVB-T2 receivers would need to include CFO compensation or correction methods for these parameters. Indeed, the carrier frequency considered in the simulation was 474 MHz, which represents the first channel from the DTT frequency range of 470 to 790 MHz assuming that the channel bandwidth is equal to 8 MHz [38]. When the carrier frequency changes from 474 MHz to 786 MHz (which represents the last carrier frequency available in the band 470–790 MHz), $\Delta f_{D_{Max}}$ is then equal to 109.16 Hz (Equation (21)) for the mobile speed of 150 km/h using Equation (12).

$$\Delta f_{D_{Max}} = \frac{150}{3.6} \times \frac{786 \times 10^6}{3 \times 10^8} = 109.16 \text{ Hz} \tag{21}$$

The normalized CFO value is equal to 0.09 using Equation (6) when the carrier frequency is 786 MHz, and the mobile speed is 150 km/h. In fact, our simulations focused on the CFO variation between 0.01 and 0.05, because above a CFO value of 0.05, the DVB-T2 system performance is very degraded. In fact, when the CFO increases above 0.05, there is enough binary or symbol errors to prevent the demodulator from performing symbol detection, the results of which would be easily exploited by the LDPC decoder for error detection and correction.

7. Conclusions and Further Work

In this paper, radiofrequency impairments were studied in digital broadcasting. Mainly, the study was focused on the CFO impact on DVB-T2 and NUCs, and UFMC-based DVB-T2 systems. As the DVB-T2 standard is mainly based on OFDM, this system suffers from some frequency offset that decreases the system performance. The study of these impairments was investigated to highlight their impact on the terrestrial digital broadcasting system DVB-T2. Moreover, UFMC and NUC techniques are advanced signal processing techniques that have shown good performance in DVB-T2. This work also studied the impact of the CFO on the system, including both NUCs and UFMC. The main results are presented as follows: UFMC-based DVB-T2 is less responsive to the CFO than the native DVB-T2 in urban environments; when NUCs are additionally used in UFMC-based DVB-T2, the same conclusion is drawn. This work gives some trends in the use of mobile reception in the DVB-T2 system. It may help broadcasters with a mobile-reception use case in their DTT networks.

One of the prospects of this work would be to obtain measurements to compare with our simulations. It could be achieved by programming software radios, such as a SDR (Software-Defined Radio) with GNU software, taking into account the transformations that we made to the native DVB-T2, and by adding the faults brought by the CFO in a synthetic way to the receiver. Then, the available system could actually measure the bit error rate and constellations, as well as the MER and EVM, even though the channel would not be representative of the TU6. In a second step, a channel synthesizer could be developed to counteract this problem. Referring to Table 3, another prospect for improving our paper would be to improve our study of the sensitivity of DVB-T2 to the CFO (either native DVB-T2, with or without UFMC, with or without rotated constellation) by treating a larger number of parameter values in the simulations, such as the size of the QAM constellation, the 2D distribution of the non-uniform constellation (NUC), the number of OFDM subcarriers, the cyclic prefix, the choice of values corresponding to the UFMC sub-band number, UFMC sub-band bandwidth, the UFMC filter length, and a choice of simulation channel other than TU6 like the “0 dB echo” channel, which corresponds to the channel used in an SFN environment. Also, the MISO technique is an optional feature of the DVB-T2 standard, but it offers a number of advantages, such as signal robustness improvement and coverage enhancement. The CFO impact on performance could be investigated in DVB-T2 and UFMC/NUC-based DVB-T2 when the MISO technique is applied. In a third step, as FBMC is a multicarrier modulation that obtained good performance in digital television systems with higher complexity, a reduced complexity version of this modulation could be studied in DVB-T2, and the CFO impact could be investigated to gather the best modulation when the CFO is considered. Finally, as a last step, the network coverage reduction induced by the CFO penalties could be computed in DVB-T2 systems, whether native or improved by NUCs or UFMC.

Author Contributions: Conceptualization, S.Z., A.-C.H., and V.M.; methodology, S.Z. and A.-C.H.; software, S.Z. and A.-C.H.; validation M.D. and V.M.; formal analysis, S.Z., A.-C.H., M.D., and V.M.; investigation, S.Z. and A.-C.H.; resources, A.-C.H.; data curation, S.Z. and A.-C.H.; writing—original draft preparation, S.Z. and A.-C.H.; writing—review and editing, A.-C.H., M.D. and V.M.; visualization, M.D. and V.M.; supervision, V.M.; project administration, M.D. and V.M.; funding acquisition, V.M. All authors have read and agreed to the published version of the manuscript.

Funding: This research was funded by ARES-CCD within the framework of the PHORAN PFS project.

Data Availability Statement: Data is contained within the article.

Acknowledgments: This work was carried out with support from the ARES-CCD within the framework of the PHORAN PFS project.

Conflicts of Interest: The authors declare no conflicts of interest. The funders had no role in the design of the study; in the collection, analyses, or interpretation of data; in the writing of the manuscript; or in the decision to publish the results.

Abbreviations

The following abbreviations are used in this manuscript:

ACI	Adjacent-Channel Interference
ATSC	Advanced Television Systems Committee
ATSC 3.0	Advanced Television Systems Committee, third generation
AWGN	Additive White Gaussian Noise
BCH	Bose–Chaudhuri–Hocquenghem
BER	Bit error rate
BICM	Bit-Interleaved Coded Modulation
CFO	Carrier frequency offset
CP	Cyclic prefix
CP-OFDM	Cyclic prefix–Orthogonal Frequency-Division Multiplexing
CR	Code rate
CRs	Code rates
DML	Deterministic maximum likelihood
DTT	Digital Terrestrial Television
DVB	Digital Video Broadcasting
DVB-H	Digital Video Broadcasting—Handset
DVB-S2	Digital Video Broadcasting Satellite, second generation
DVB-T	Digital Video Broadcasting—Terrestrial, first generation
DVB-T2	Digital Video Broadcasting—Terrestrial, second generation
ETSI	European Telecommunications Standards Institute
EVM	Error Vector Magnitude
F-OFDM	Filtered-Orthogonal Frequency-Division Multiplexing
FBMC	Filter Bank Multicarrier
FEC	Forward Error Correction
FFT	Fast Fourier Transform
GFDM	Generalized Frequency-Division Multiplexing
HDTV	High-Definition Television
ICI	Intercarrier Interference
IFFT	Inverse Fast Fourier Transform
ISI	Intersymbol Interference
ITU	International Telecommunication Union
LDPC	Low-Density Parity Check
LLR	Log-Likelihood Ratio
LoS	Line of sight
LTE	Long-Term Evolution

MDPI	Multidisciplinary Digital Publishing Institute
MER	Modulation Error Ratio
MIMO	Multiple-Input Multiple-Output
MISO	Multiple-Input Signal-Output
ML	Maximum likelihood
MMSE	Minimum Mean Square Error
MSE	Mean Square Error
NUC	Non-uniform constellation
NUCs	Non-uniform constellations
OFDM	Orthogonal Frequency-Division Multiplexing
OOB	Out Of Band
PDP	Power Delay Profile
QAM	Quadrature Amplitude Modulation
SFN	Single-Frequency Network
SFO	Sampling frequency offset
SINR	Signal-to-interference-plus-noise ratio
SISO	Single-Input Single-Output
SML	Stochastic maximum likelihood
SNR	Signal-to-Noise Ratio
SLL	Side-Lobe Level
TPS	Transmission Parameters Signaling
TU6	Typical Urban 6
TV	Television
UFMC	Universal Filtered Multicarrier
UHD	Ultrahigh Definition
VLC	Visible-Light Communication
ZF	Zero forcing

References

1. Zhang, X.; Liu, J.; Li, H.; Himed B. Maximum Likelihood Synchronization for DVB-T2 in Unknown Fading Channels. *IEEE Trans. Broadcast.* **2015**, *61*, 615–623.
2. European Broadcasting Union. *Digital Video Broadcasting (DVB); Frame Structure Channel Coding and Modulation for a Second Generation Digital Terrestrial Television Broadcasting Systems (DVB-T2)*; ETSI EN 302 755 V1.4.1; European Telecommunications Standards Institute (ETSI): Sophia-Antipolis, France, 2015; pp. 1–188.
3. Jeon, E.-S.; Seo, J.-W.; Yang, J.-H.; Paik, J.-H.; Kim, D.-K. Iterative Detection and ICI Cancellation for MISO-mode DVB-T2 System with Dual Carrier Frequency Offsets. *KSII Trans. Internet Inf. Syst.* **2012**, *6*, 702–721.
4. Zhang, X.; Bie, H.; Lei; C.; Zheng, J. A Robust Timing and Frequency Synchronization Scheme for DVB-T2 system. In Proceedings of the IEEE 81st Vehicular Technology Conference (VTC Spring), Glasgow, UK, 11–14 May 2015.
5. Timo, R.; Koivunen V. Carrier Frequency Synchronization for Mobile Television Receivers. In Proceedings of the IEEE International Symposium on Circuits and Systems (ISCAS), New Orleans, LA, USA, 27–30 May 2007; pp. 261–264.
6. Rotoloni, M.; Tomasin, S.; Vangelista, L. On correlation-based synchronization for DVB-T2. *IEEE Commun. Lett.* **2010**, *14*, 248–250.
7. Rotoloni, M.; Tomasin, S.; Vangelista, L. Maximum Likelihood Estimation of Time and Carrier Frequency Offset for DVB-T2. *IEEE Trans. Broadcast.* **2012**, *58*, 77–86.
8. Baek, J.-S.; Seo, J.-S. Effective symbol timing recovery based on pilot-aided channel estimation for MISO transmission mode of DVB-T2 system. *IEEE Trans. Broadcast.* **2010**, *56*, 193–200.
9. Honfoga, A.-C.; Dossou, M.; Moeyaert, V. Performance Comparison of New Waveforms Applied to DVB-T2 Transmissions. In Proceedings of the IEEE International Symposium on Broadband Multimedia Systems and Broadcasting (BMSB), Paris, France, 27–29 October 2020.
10. Shatrughna, P.Y. Performance Optimization of Universal Filtered Multicarrier Technique for Next Generation Communication Systems. *Int. J. Electr. Comput. Eng. Syst.* **2023**, *14*, 119–127.
11. Georlette, V.; Honfoga, A.-C.; Dossou, M.; Moeyaert, V. Exploring Universal Filtered Multi Carrier Waveform for Last Meter Connectivity in 6G: A Street-Lighting-Driven Approach with Enhanced Simulator for IoT Application Dimensioning. *Future Internet* **2024**, *16*, 112–125.
12. European Broadcasting Union. *Digital Video Broadcasting (DVB); Framing Structure, Channel Coding and Modulation for Digital Terrestrial Television (DVB-T)*; ETSI EN 300 744; Technical Report; European Telecommunications Standards Institute (ETSI): Sophia-Antipolis, France, 2015; pp. 1–66.
13. Georlette, V.; Moeyaert V. Li-Fi and Visible Light Communication for Smart Cities and Industry 4.0: Challenges, research & market status in 2023. In Proceedings of the IEEE 23rd International Conference on Transparent Optical Networks (ICTON), Bucharest, Romania, 2–6 July 2023.

14. Tognissè, I.S.; Kora, A.D.; Degila, J. Infrastructure Sharing Model To Connect The Unconnected In Rural Areas. *Itu J. Future Evol. Technol.* **2021**, *2*, 1–10.
15. European Broadcasting Union (EBU). *Compatibility Between 5G Broadcast and Other DTT Systems in the Sub-700 Mhz Band*; TR 064, Technical Report; EBU: Geneva, Switzerland, 2021; pp. 1–47.
16. Arndt, D.M.; da Rocha, C.A. Performance Comparison Between OFDM and FBMC Systems in Digital TV Transmission. In Proceedings of the IEEE Third Latin-American Conference on Communications, Belem, Brazil, 24–26 October 2011.
17. Honfoga, A.-C.; Nguyen, T.T.; Dossou, M.; Moeyaert, V. Application of FBMC to DVB-T2: A Comparison vs. Classical OFDM Transmissions. In Proceedings of the IEEE GlobalSIP conference, Ottawa, ON, Canada, 11–14 November 2019.
18. Honfoga, A.-C.; Dossou, M.; Dassi, P.; Moeyaert, V. Filtered Based UFMC Waveform Applied on Joint DVB-T2/NUC System. In Proceedings of the EAI AFRICOMM—12th EAI International Conference on e-Infrastructure and e-Services for Developing Countries, Ebène City, Mauritius, 2–4 December 2020.
19. Honfoga, A.-C.; Dossou, M.; Moeyaert, V. Complexity Analysis on 5G Candidate Waveforms for DVB-T2: A survey. In Proceedings of the IEEE 4th International Conference on Advanced Communication Technologies and Networking (Commnet), Rabat, Morocco, 3–5 December 2021.
20. Fitriyani, D.; Anwar, K.; Saputri, D. Study on Radio Frequency Profile of Indonesia Digital Television DVB-T2 for Urban Areas. In Proceedings of the 1st International Conference on Islam, Science and Technology, Bandung, Indonesia, ICONISTECH 2019, 11–12 July 2019.
21. Agustin, R.D.; Astawa, I.G.P.; Pratiarso, A. Performance Analysis of Turbo Coding Implementation in MIMO Based DVB-T2 System. In Proceedings of the IEEE International Electronics Symposium (IES), Surabaya, Indonesia, 29–30 September 2020; pp. 179–183.
22. Chakiki, M.A.F.; Astawa, I.G.P.; Budikarso, A. Performance Analysis of DVB-T2 System Based on MIMO Using Low Density Parity Check (LDPC) Code Technique and Maximum Likelihood (ML) Detection. In Proceedings of the IEEE International Electronics Symposium (IES), Surabaya, Indonesia, 29–30 September 2020; pp. 169–173.
23. Tarigan, N.Y.; Pamungkas, W.; Isnawati, A.F. Performance of DVB-T2 Application in High-Speed Train Transportation System. *Eng. Technol. Appl. Sci. Res.* **2024**, *14*, 17084–17090.
24. Defeng, H.; Letaief, K.B. Carrier Frequency Offset Estimation for OFDM Systems Using Null Subcarriers. *IEEE Trans. Commun.* **2006**, *54*, 813–823.
25. Aziz, W.; Ahmed, E.; Abbas, G.; Saleem, S.; Islam Q. Performance analysis of carrier frequency offset (CFO) in OFDM using MATLAB. *J. Eng.* **2012**, *1*, 5–10.
26. Almradi, A.; Hamdi, K.A. Spectral efficiency of OFDM systems with random residual CFO. *IEEE Trans. Commun.* **2015**, *63*, 2580–2590.
27. Sathiyapriya, N.S. Implementation and study of universal filtered multi carrier under carrier frequency offset for 5G. *Int. J. Electron. Commun.* **2016**, *4*, 1–5.
28. Padmavathi, T.; Udayasree, P.; Kusumakumari, Ch.; Madhu, R. Performance of Universal Filter Multi Carrier in the presence of Carrier Frequency Offset. In Proceedings of the IEEE International Conference on Wireless Communications, Signal Processing and Networking (WiSPNET), Chennai, India, 22–24 March 2017.
29. Choi, K. FD-FBMC: A Solution for Multicarrier Full Duplex Cellular Systems. *IEEE Commun. Lett.* **2021**, *25*, 617–621.
30. Schaich, F.; Wild, T. Waveform contenders for 5G—OFDM vs. FBMC vs. UFMC. In Proceedings of the IEEE 6th International Symposium on Communications, Control and Signal Processing (ISCCSP), Athens, Greece, 21–23 May 2014.
31. Fuentes, M.; Mi, D.; Chen H.; Garro E.; Luis Carcel, J.; David, V.; Mouhouche, B.; Gomez-Barquero D. Physical layer performance evaluation of LTE-advanced pro broadcast and ATSC 3.0 systems. *IEEE Trans. Broadcast.* **2019**, *65*, 477–488.
32. Barrueco, J.; Montalban, J.; Iradier, E.; Angueira, P. Constellation design for future communication systems: A comprehensive survey. *IEEE Access* **2021**, *9*, 89778–89797.
33. Advanced Television Systems Committee. *ATSC Physical Layer Protocol, Next Generation Broadcasting System to Handheld*; Document A/322; Advanced Television Systems Committee: Washington, DC, USA, 2024; pp. 1–263.
34. Smaini, L. *RF Analog Impairments Modeling for Communication Systems Simulation: Application to OFDM-Based Transceivers*; John Wiley & Sons: Hoboken, NJ, USA, 2012.
35. Fisher, W. *Digital Video and Audio Broadcasting. A Practical Engineering Guide*, 4th ed.; Springer: Berlin/Heidelberg, Germany, 2020.
36. Rohde and Schwarz, Fading Channel Simulation in DVB, Broadcasting division, Application note, 7BM05_1E, 2001.
37. ITU. *Digital Dividend: Insights for Spectrum Decisions*; Telecommunication Development Sector: Geneva, Switzerland, 2012.
38. ITU. *Frequency and Network Planning Aspects of DVB-T2*; Broadcasting Service (Television); Radio Communication Sector: Geneva, Switzerland, 2020.
39. DVB-T2 Reference Streams (T2StreamsParameterSets84.xlsx). Available online: https://dvb.org/specifications/verification-validation/dvb-t2-reference-streams/ (accessed on 11 November 2024).
40. Gallager, R. Low-density parity-check codes. *IRE Trans. Inf. Theory* **1962**, *8*, 21–28.
41. Low-Density Parity-Check (LDPC) Codes from DVB-S2 Standard. Available online: https://www.mathworks.com/help/comm/ref/dvbs2ldpc.html (accessed on 12 November 2024).
42. Manda, R.; Gowri, R. A Method to Reduce the Effect of Inter-Sub-Band Interference (ISBI) and Inter Carrier Interference (ICI) in UFMC. In *Intelligent Communication, Control and Devices, Proceedings of ICICCD*; Springer: Singapore, 2018; pp. 921–933.

43. European Broadcasting Union. *Digital Video Broadcasting (DVB); Measurement Guidelines for DVB Systems*; ETSI TR 101 290 V1.4.1; European Telecommunications Standards Institute (ETSI): Sophia-Antipolis, France, 2020; pp. 1–174.
44. Rugini, L.; Banelli, P. BER of OFDM systems impaired by carrier frequency offset in multipath fading channels. *IEEE Trans. Wirel. Commun.* **2005**, *4*, 2279–2288.
45. European Broadcasting Union. *Digital Video Broadcasting (DVB); Implementation Guidelines for a Second Generation Digital Terrestrial Television Broadcasting System (DVB-T2)*; ETSI TS 102 831 V1.2.1; European Telecommunications Standards Institute (ETSI): Sophia-Antipolis, France, 2012; pp. 1–244.
46. Marchand C. Implementation of an LDPC Decoder for the DVB-S2,-T2 and-C2 Standards. Ph.D. Thesis, Université de Bretagne Sud, Lorient, France, 2015.